The Astronomical Journal, 158:35 (27pp), 2019 July https://doi.org/10.3847/1538-3881/ab21e1

The *Swift* UVOT Stars Survey. III. Photometry and Color–Magnitude Diagrams of 103 Galactic Open Clusters

Michael H. Siegel[1], Samuel J. LaPorte[1], Blair L. Porterfield[1,2], Lea M. Z. Hagen[1,2,3], and Caryl A. Gronwall[1,2]
[1] Pennsylvania State University, Department of Astronomy, 525 Davey Laboratory, University Park, PA 16802, USA; mhs18@psu.edu, sjl5346@psu.edu, blp14@psu.edu, lmz5057@psu.edu, cag18@psu.edu
[2] Institute for Gravitation and the Cosmos, Pennsylvania State University, University Park, PA 16802, USA
[3] Space Telescope Science Institute, 3700 San Martin Drive, Baltimore, MD 21218, USA; bporterfield@stsci.edu, lhagen@stsci.edu
Received 2019 March 11; revised 2019 May 3; accepted 2019 May 6; published 2019 July 1

Abstract

As part of the *Swift*/Ultraviolet-Optical Telescope Stars Survey, we present near-ultraviolet (NUV; 3000–1700 Å) point-source photometry for 103 Galactic open clusters. These data, taken over the span of the mission, provide a unique and unprecedented set of NUV point-source photometry on simple stellar populations. After applying a membership analysis fueled mostly by *Gaia* DR2 proper motions, we find that 49 of these 103 have clear precise color–magnitude diagrams (CMDs) amenable to investigation. We compare the CMDs to theoretical isochrones and find good agreement between the theoretical isochrones and the CMDs. The exceptions are the fainter parts of the main sequence and the red giant branch in the *uvw*2 − *uvw*1 CMDs, which is most likely due to either the difficulty of correcting for the red leak in the *uvw*2 filter or limitations in our understanding of UV opacities for cool stars. For the most part, our derived cluster parameters—age, distance, and reddening—agree with the consensus literature, but we find a few clusters that warrant substantial revision from literature values, notably NGC 2304, NGC 2343, NGC 2360, NGC 2396, NGC 2428, NGC 2509, NGC 2533, NGC 2571, NGC 2818, Collinder 220, and NGC 6939. A number of these are clusters in the third Galactic quadrant, where previous studies may have mistaken the disk sequence for the cluster. However, the *Gaia* DR2 proper motions clearly favor a different sequence. A number of clusters also show white dwarf and blue straggler sequences. We confirm the presence of extended main-sequence turnoffs in NGC 2360 and NGC 2818 and show hints of them in a number of other clusters that may warrant future spectroscopic study. Most of the clusters in the study have low extinction, and the rest are well fit by a "Milky Way–like" extinction law. However, Collinder 220 hints at a possible "LMC-like" extinction law. We finally provide a comprehensive point-source catalog to the community as a tool for future investigation.

Key words: open clusters and associations: general – stars: early-type – stars: general

Supporting material: machine-readable tables

1. Introduction

Open clusters are gravitationally bound collections of 10^2–10^4 stars born in the same star formation event. They are, by far, the most abundant family of clusters in the Milky Way, with over 1500 cluster or cluster candidates having been cataloged (Dias et al. 2002) Galactic open clusters are predominantly young and metal-rich—most of the older clusters having long since dissolved into the Galactic field. However, a number of old and metal-poor clusters have been detected and serve as "fossils" for studying the early Galaxy.

As compact collections of stars of similar age, abundance, distance, and reddening, individual star clusters present a snapshot of stellar evolution. Studying large samples of clusters allows us to piece together the narrative of stellar evolution and constrain the photometric properties of stars as functions of mass, age, and chemistry. Much of our understanding of stellar evolution and photometry comes from the study of Galactic open and globular star clusters. Cluster of all ages and chemistries are known to host stars that are bright in the ultraviolet (UV), as shown in Siegel et al. (2014, hereafter Paper I). These UV-bright stars in the nearby universe have counterparts in the UV-bright stars seen in nearby galaxies and are, ultimately, parallels to the stars contributing to the UV light of distant unresolved stellar populations. Any understanding of luminous hot UV-bright stars and stellar populations dominated by them will therefore have to lay its foundation on the study of nearby star clusters. They are not only the best repositories in which to find such stars, but having found them, the properties can be immediately connected with stellar populations of known age, distance, reddening, and chemistry.

The study of the UV properties of star clusters is still in its early stages, as detailed in Paper I. But there are a number of recent results that indicate that this is a fertile field of study. For example, studies of open clusters in the Magellanic Clouds have shown complex structure in the main-sequence turnoff (MSTO)—an extended MSTO (eMSTO) and split MSTOs (Mackey & Broby Nielsen 2007; Milone et al. 2009; Goudfrooij et al. 2011). This split has also recently been identified in a number of Galactic clusters (Cordoni et al. 2018; Marino et al. 2018). This fine structure is thought to the be the result of stellar rotation, which can affect the evolutionary lifetimes of stars and may show up more clearly in the UV. A recent comprehensive study of M67 (Sindhu et al. 2018) identified numerous blue straggler stars (BSSs), white dwarf binaries, and stars that had excess far-UV emission consistent with either unresolved binarism or chromospheric activity.

In addition to their utility for studying stellar evolution and the properties of rare phases of stellar evolution, Galactic open clusters can be used as the building blocks for studying larger astrophysical questions. Open clusters, for example, can be

used to probe the chemodynamical properties of the Galactic disk (see, e.g., Friel 1995; Twarog et al. 1997; Yong et al. 2005, 2012; Frinchaboy & Majewski 2008). Old open clusters, with ages greater than 1 Gyr, are particularly suited to tracing the chemical evolution of the disk through their age–metallicity relationship (AMR). Indeed, the similarity between the AMR of a small group of open clusters and that of merging dwarf galaxy systems has been key to confirming past Galactic mergers (Frinchaboy et al. 2006). Open clusters may be particularly useful for probing the UV extinction properties of nearby dust. As we have noted before (Paper I; Hagen et al. 2017, 2019), the UV extinction curve is uncertain both in slope and in the strength of the "blue bump" at 2175 Å (Stecher 1965; Seaton 1979; Gordon et al. 2003). Open clusters can serve as probes of dust properties on small and large scales.

Of particular interest to recent scientific investigations is the utility of clusters for studying the properties of complex stellar populations. Open clusters are nearby, meaning they can be probed on a star-by-star basis to determine age, abundance, foreground reddening, and distance. However, they can also be studied through their *integrated light*. By combining these two measures, one can calibrate the study of more distant stellar populations that cannot be resolved on a star-by-star basis but can only be studied through the properties of their integrated light (an illustration of this in the context of the Magellanic Clouds can be found in Searle et al. 1980). Studies of the integrated light of unresolved stellar populations have proven extraordinarily useful for untangling the star formation histories and dust extinction properties of both nearby and distant galaxies (see, e.g., Hoversten et al. 2011; Calzetti et al. 2015; Hagen et al. 2017, 2019). However, these studies have a limitation: the UV portion of the spectral energy distribution is not as well constrained as the optical and infrared. The lack of empirical information needed to calibrate the synthetic spectra of unresolved stellar populations was specifically cited by Bruzual (2009) as a limitation on the utility of the models.

Despite the tremendous efforts made by investigators, most of the Milky Way's open clusters have not been studied in great detail at any wavelength. The sheer number of open clusters in the Galaxy precludes most from being targeted for individual study. Indeed, many of the parameters used by the WEBDA online database of open clusters[4] come from global optical-infrared (OIR) surveys of hundreds of clusters, such as that of Kharchenko et al. (2013, 2016, hereafter K13 and K16, respectively). But there are additional issues that complicate the study of open clusters, most notably their preferred location within the Galactic midplane, with concomitant heavy foreground reddening and field star contamination.

This deficit of individual study is particularly acute in the UV, where very few clusters have been studied in detail (see discussion in Paper I). This lacuna is the natural apotheosis of the factors that limit their study in the optical: their location within the Galactic midplane makes study difficult due to either crowding (most previous UV missions had coarse spatial resolution), field star contamination, foreground extinction (which is much stronger in the UV), or simple brightness constraints that preclude missions like the *Galaxy Evolution Explorer* (*GALEX*) from studying objects in the Galactic midplane.

[4] http://www.univie.ac.at/webda/

As a result of this, the spectral synthesis models used to study distant unresolved stellar populations are still not well constrained in the UV. And this is particularly problematic because young stellar populations—those most visible over the long distances in extragalactic astronomy and cosmology—emit a large fraction of their rest-frame light in the UV. The lack of thorough, systematic, and empirical study of young UV-bright stellar populations is a significant and limiting problem for extant and planned UV surveys of the Milky Way, the Magellanic Clouds, Local Group objects, nearby galaxies, and distant galaxies. Understanding the star-by-star and integral photometry of distant and extragalactic systems—from the nearby to the deep universe—is critically dependent on studies of nearby open clusters.

In this contribution, we address this deficit in our knowledge of Galactic open clusters with a survey of 103 open clusters observed in the near-UV (NUV) with the *Neil Gehrels Swift* mission's Ultraviolet-Optical Telescope (UVOT). By combining *Swift*'s wide-field moderate-resolution photometry with precise astrometry from the recent *Gaia* Data Release 2 (DR2) catalog, we are able to study these clusters in unprecedented detail, testing the utility of theoretical isochrones and either confirming or revising the literature parameters for these clusters.

We present the observational details of the program in Section 2. We then detail the limitations on our analysis produced by saturation of the brightest stars and contamination from the Galactic disk in Section 3. Using some radial velocities, but mostly *Gaia* DR2 proper motions, to establish membership, we are able to identify 49 clusters that have clear and distinct color–magnitude sequences, many of which have never been the target of detailed study. We present these color–magnitude diagrams (CMDs) along with a comparison to the theoretical isochrones with which we measure or revise their fundamental properties. The resultant test of the theoretical isochrones shows excellent agreement, indicating that the models perform well in the UV. We show that the isochrones have a tendency to not match the photometry of cooler stars—red giant branch (RGB) and late-type main sequence (MS) stars. We finally look ahead to other uses for this data set, which we will provide to the community.

2. Observations and Data Reductions

2.1. UVOT Data

The UVOT is a modified Richey–Chretien 30 cm telescope that has a wide ($17' \times 17'$) field of view and a microchannel plate intensified CCD operating in photon-counting mode (see details in Roming et al. 2000, 2004, 2005) on board the *Neil Gehrels Swift* Gamma Ray Burst Mission (Gehrels et al. 2004). The instrument is equipped with a filter wheel that includes a clear white filter; *u*, *b*, and *v* optical filters; *uvw*1, *uvm*2, and *uvw*2 UV filters; a magnifier; two grisms; and a blocked filter. Although its primary mission is to measure the optical/UV afterglows of gamma-ray bursts, the wide field, $2\farcs3$ resolution, broad wavelength range (1700–8000 Å), and ability to observe simultaneously with *Swift*'s X-ray Telescope (Burrows et al. 2005) allow a broad range of science, including the study of hot or highly energetic stars. It is particularly ideal, in the context of hot stars, for studying nearby star clusters. Its wide field can enclose most nearby open clusters in a single pointing, and its resolution allows the measurement of stars almost to the center

Table 1
Swift/UVOT Observations of Open Clusters

Cluster	*u* Exp. Time (ks)	*uvw1* Exp. Time (ks)	*uvm2* Exp. Time (ks)	*uvw2* Exp. Time (ks)	Observation Dates
Blanco 1	0	3378	2461	3071	2010 Nov 10–2011 Jan 25
NGC 188	1195	2842	3111	4555	2005 Jun 29
…	…	…	…	…	2005 Oct 13
…	…	…	…	…	2007 Oct 30–2007 Dec 6
NGC 752	0	798	1032	1076	2011 Jul 31–2011 Sep 6
IC 1805	0	862	926	926	2008 Apr 6
NGC 1039 (M34)	0	2137	2206	2206	2011 Mar 8
…	…	…	…	…	2011 Jul 10–2011 Jul 14
NGC 1896	0	1717	1614	1614	2013 Oct 27
NGC 1996	0	3490	3428	3507	2013 Oct 20–2013 Oct 26

(This table is available in its entirety in machine-readable form.)

of the most crowded fields. The NUV filters—with effective wavelengths of 2600, 2246, and 1928 Å for *uvw*1, *uvm*2, and *uvw*2, respectively—provide good coverage of the NUV wavelength range and sensitivity to the 2175 Å blue bump.

The open clusters surveyed by UVOT are drawn from a variety of programs. The bulk was imaged as part of M. Siegel's approved Cycle 12 GI and team fill-in programs, observed optimally for 6 ks in UVOT's three NUV filters (although, in practice, the observing time tended to be closer to 5 ks). Others were observed as calibration targets or coincidentally with other studies. We have included clusters in the sample if they were observed for at least 0.8 ks in two of UVOT's three NUV filters and where the field center was within 5′ of the nominal cluster center, although some exceptions have been made to expand the sample. The clusters in our GI and fill-in program were generally selected to be comparable to the UVOT field of view, with low reddening ($E\,(B-V) < 0.5$) and locations away from the Galactic center region, which is the most heavily oversubscribed part of the sky for *Swift* observations.

The list of 103 clusters is given in Table 1. The table lists the exposure time in UVOT's three NUV passbands, as well as its broadband *u* passband. All exposure times are given as the maximum exposure time on the combined image, which removes dead-time losses. Most of the cluster images were created by combining any image within 7.′5 of the cluster center. However, some of the first images processed in the program used a much larger search radius in an effort to provide data on the clusters with the richest history of prior observations. All clusters were processed and photometered through the pipeline described in Paper I, updated to the most recent calibrations (Breeveld et al. 2011).

While this particular contribution focuses on the clusters with the cleanest CMDs, we have created photometric catalogs for all 103 clusters. The photometric catalogs include calibrated point-spread function (PSF) photometry in all available passbands, including broadband *b* and *v* when available. They have been filtered of objects with DAOPHOT (Stetson 1987, 1994) structural parameters of $|SHARP| > 0.5$ to remove blends and detections near bright saturated stars (see Paper I for more information). The catalogs are currently available on request but will eventually be made available through the Mikulski Archive for Space Telescopes.

Of the clusters in the sample, all but one have *uvw*1 data, all but one have *uvm*2 data, and all but three have *uvw*2 data. Only two clusters—Hogg 16 and Westerlund 2—lack *uvm*2 and *uvw*1 data. Our sample includes few clusters with very young ages ($t < 100$ Myr). The reason for this is that very young clusters tend to be either far too bright or far too enshrouded in dust for UVOT study.

3. Analysis and Results

3.1. Bright Star Issues

Most of our cluster fields are close to or within the Galactic midplane. They also tend to be young ($t < 1$ Gyr) and nearby ($m - M < 14$). As a result, a number of cluster fields have numerous bright saturated stars. "Saturated," in the case of a photon-counting instrument like UVOT, does not mean "saturated" in the same sense as a CCD detector. What this means is that the incident count rate exceeds 372 s^{-1}, the limit at which UVOT can no longer count incident photons (corresponding to AB magnitudes of 12.52, 12.11, and 12.68 in the *uvw*1, *uvm*2, and *uvw*2 filters, respectively). Thus, only crude lower limits can be applied to the brightness of these stars. Even before reaching such a high level, however, the coincidence loss becomes very strong, and the dead time of the detector for incident photons will result in dark boxes around the saturated cores of bright stars (Poole et al. 2008). This lowers the limit at which useful photometry can be measured to well below 372 s^{-1}. This is particularly noticeable with PSF photometry, as very high coincidence loss both changes the shape of the PSF for bright stars and can cause DAOPHOT to underestimate the background sky level. In the discussions below, the phrase "saturated" stars will be applied to both contexts and has the general meaning of a star whose coincidence loss is too strong for reliable PSF photometry. While Page et al. (2017) recently outlined a method to measure photometry from saturated stars using readout streaks, this method was not appropriate for most of our saturated stars, as it would not produce the precision needed to constrain theoretical isochrones. We have noted within the text several clusters where the bright end of the MS is saturated, and we can only

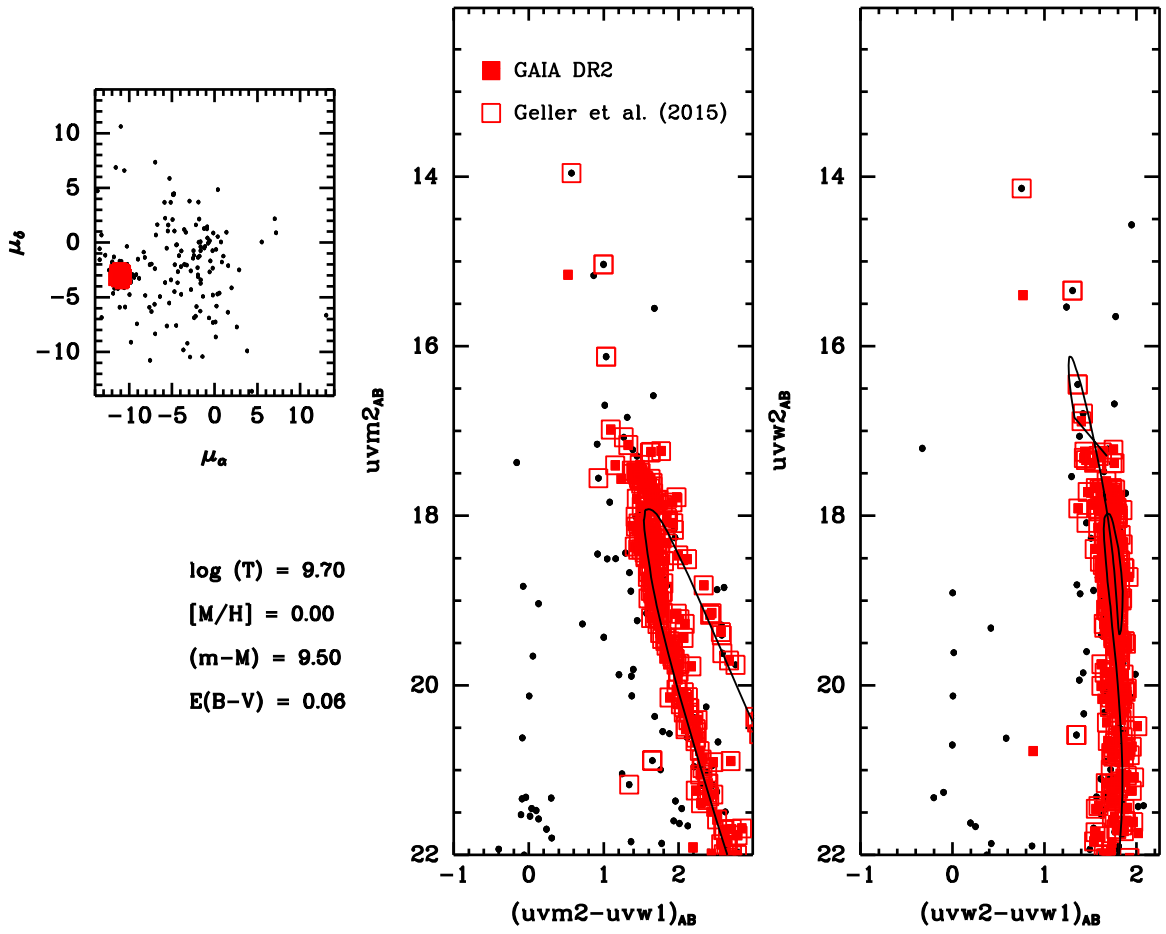

Figure 1. *Gaia* DR2 VPD and *Swift*/UVOT CMDs of the old open cluster M67 compared the PARSEC-COLIBRI isochrones fit in Paper I. The filled red squares show astrometric members selected from *Gaia* DR2, while the open red squares show radial velocity members selected from Geller et al. (2015).

provide upper limits on the age of the clusters. Two clusters that were observed for our program—NGC 2547 and NGC 2516—are not included in the sample of 103 presented here because of bright star contamination problems that made photometry of any kind impossible.

The other complication of bright stars is that they produce diffuse light that may affect photometry (see extended discussion in the context of M31 in Hagen et al. 2019). This can include internal reflections, donuts, and readout lines. However, while scattered light is a problem for the photometry of extended sources, we have not found it to be a problem for point sources, which are measured from a local sky. Our comparison of UVOT photon-counting photometry to ground-based CCD photometry in Paper I showed that our methods produce reliable linear photometry for all but the brightest stars.

3.2. Cluster Membership

While some of the clusters in our sample—such as M67—are above the Galactic plane, the vast majority are within the plane ($|b| < 10$). This can create a problem in that the Galactic field star population is very populous in these fields, potentially overwhelming the cluster population or confounding analysis of its color–magnitude sequence. In some fields, the correlation between distance/reddening/age causes the field stars to vaguely resemble an MS (see, e.g., NGC 2360 in Section 3.4.13). And even in the most spartan fields, it is difficult to identify rare phases of stellar evolution, such as blue stragglers or white dwarfs, based on photometry alone.

We approached this problem on several fronts. Earlier proper-motion samples proved too imprecise in most cases, as the cluster proper motions were within the field star distribution and the studies lacked the precision to tease them out. Spatial analysis—using the parameters of K16 to select stars within the core or half-light radii—proved effective for massive clusters but not for small ones. Radial velocity surveys, such as that of Mermilliod et al. (2008, hereafter MMU), proved useful but were rarely extensive enough to cover much of the cluster and were primarily focused on bright red RGB stars. Such stars are ideal for optical studies but faint and poorly constrained in the UV.

Ultimately, we settled on using the proper-motion data provided in the recent *Gaia* DR2 (Gaia Collaboration 2016, 2018). The *Gaia* data are uniform and precise and have a depth similar to that of UVOT. Cantat-Gaudin et al. (2018, hereafter CG18) recently published a comprehensive membership analysis of 1212 clusters—including almost all of our program clusters—using five-dimensional phase-space information. We have used their membership analysis for cluster membership in the UVOT data, identifying as members stars with probabilities greater than 90%. For a handful of clusters, however, we found that the CG18 study only identified a small number of member stars. For these clusters, we did our own membership analysis, as detailed in the text.

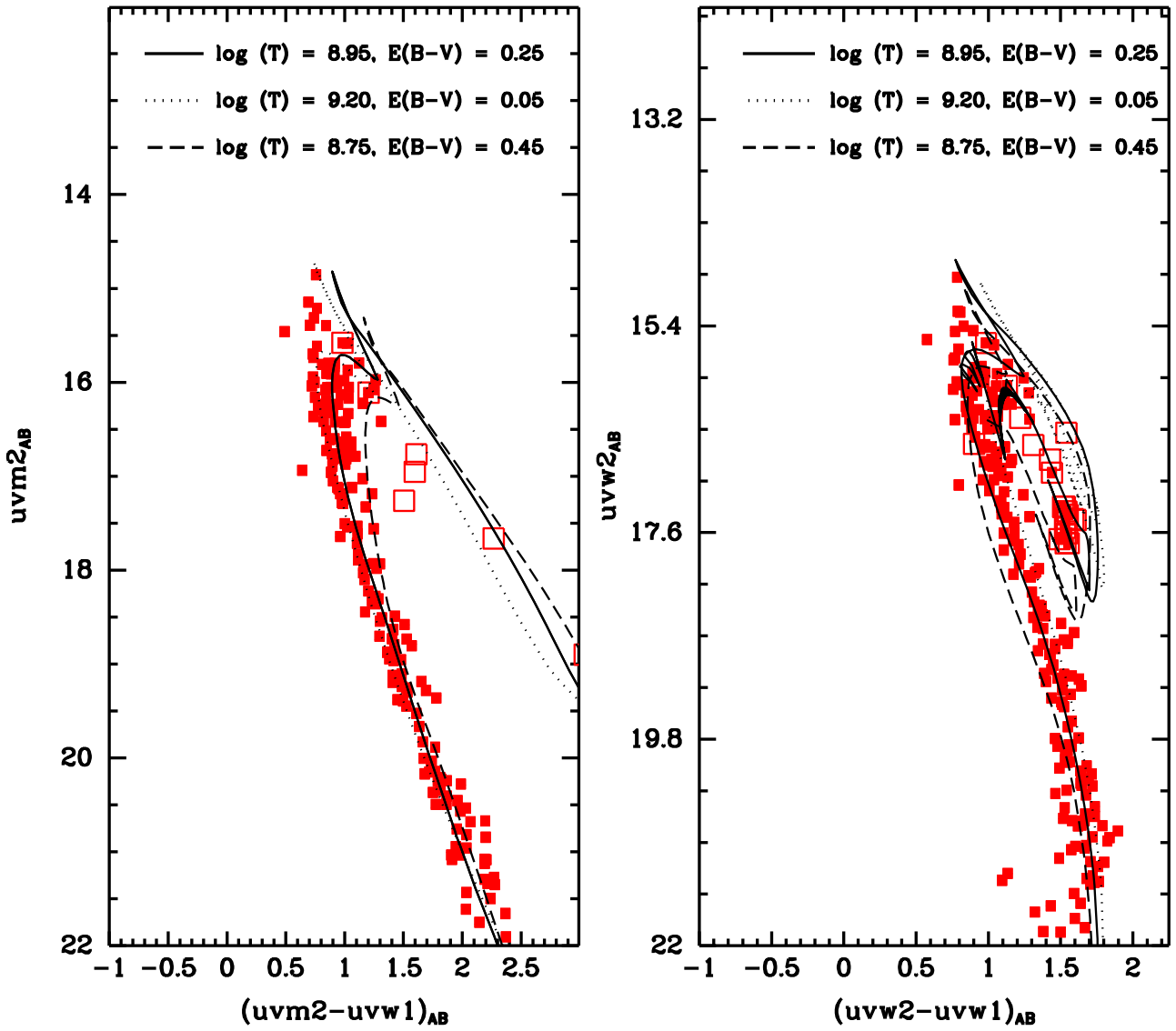

Figure 2. Comparison of different isochrone fits to the photometry of the globular cluster NGC 2360. The three lines are all set at a metallicity of [M/H] = −0.1 and a distance modulus of $m - M = 10.05$. However, they are set at different reddening values, with age adjusted to better match the MSTO. Note that increasing or decreasing the reddening has opposite effects in the two CMDs. A lower (higher) reddening moves the isochrone below (above) the observed MS in the $uvm2 - uvw1$ CMD and above (below) in the $uvw2 - uvw1$ CMD. This allows the reddening to be easily constrained by the observational data.

Figure 1 demonstrates the utility of the *Gaia* data in the context of M67. The left panel shows a vector-point diagram (VPD) of the M67 field. The dispersed population toward the center is the Galactic disk, while the concentrated group of points off center is the cluster. Almost all of the radial velocity members from the recent survey of Geller et al. (2015) land within the offset clump. For the majority of the open clusters, the separation between cluster and field was not quite so dramatic. More often, the cluster proper motion was within the field star distribution. However, the *Gaia* DR2 parallaxes and proper motions are so precise that the cluster members are steadily readily identified as a very tight clump of stars within the more dispersed Galactic background. This allows them to be easily disentangled from the field star population with high confidence.

After extensive analysis, we found that 49 of our 103 target clusters could easily be distinguished from the field star population and showed a clear sequence in the CMDs. We note that there are a number of clusters that show clear clumps of cluster stars in the *Gaia* data themselves but fail to cross-match enough stars to the UVOT data for analysis because the clusters are either too faint or too spatially dispersed. The photometry catalogs included all photometric measures for both members and nonmembers.

3.3. Isochrone Fitting and Analysis

The goal of this paper is to compare the point-source photometry of the clusters to theoretical isochrones in order to test the utility of the isochrones (and, by extension, the atmospheric models underpinning them) in the context of young to intermediate-age stellar populations. The isochrones chosen for this exercise are the PARSEC-COLIBRI isochrones of Marigo et al. (2017, hereafter M17). These isochrones cover the entire range of ages and metallicities of the open cluster sample. The most significant revisions of this iteration are to the thermally pulsing asymptotic giant branch (TP-AGB), which is not relevant to our analysis, as these stars are too cool for good constraint with UVOT. In fact, the detailed treatment

Table 2
Parameters of Clusters in This Study

Cluster	Distance m–M	$E\,(B-V)$	log(Age) (yr)	[Fe/H]	Source
NGC 752	8.30	0.03	9.15	−0.03	Böcek Topcu et al. (2015), Twarog et al. (2015)
NGC 752	8.30	0.05	9.15	+0.00	This study
NGC 1039	8.38	0.10	8.35	+0.07	Jones & Prosser (1996)
NGC 1039	8.71	0.07	8.25	+0.07	Schuler et al. (2003)
NGC 1039	8.54	0.08	8.38	0.07	Kharchenko et al. (2013)
NGC 1039	8.75	0.10	<8.20	+0.10	This study
NGC 2192	12.70	0.20	9.04	−0.31	Park & Lee (1999)
NGC 2192	12.70	0.16	9.15	−0.31	Tapia et al. (2010)
NGC 2192	12.70	0.15	9.20	−0.30	This study
NGC 2204	13.00	0.13	9.20	−0.23	Kassis et al. (1997), Jacobson et al. (2011)
NGC 2204	13.16	0.00	9.35	−0.20	This study
NGC 2243	12.78	0.11	9.67	−0.42	Twarog et al. (1997), Jacobson et al. (2011)
NGC 2243	12.91	0.00	9.70	−0.50	This study
NGC 2251	10.60	0.20	8.50	−0.10	Parisi et al. (2005), Reddy et al. (2013)
NGC 2251	10.61	0.25	8.55	−0.10	This study
NGC 2281	8.55	0.09	8.80	0.00	Glaspey (1987), Netopil (2017)
NGC 2281	8.56	0.15	8.80	0.00	This study

Note.
[a] Using LMC extinction law.

(This table is available in its entirety in machine-readable form.)

of this phase causes the isochrones to loop around as the theoretical stars' UV emission (actually, their red leak into the UV passbands; see the Appendix to Paper I) waxes and wanes during their TP-AGB phases. For the figures below, the TP-AGB phase has been removed from the isochrones for the sake of clarity.

Isochrones were initially laid down using literature values from studies specific to the individual cluster, if possible, and from K16 where no previous focused study had been made. The isochrones were then adjusted interactively to better overlap the *Gaia*-selected sequences, with variation allowed in age, metallicity, reddening, distance, and reddening law (either Galactic, SMC, or LMC, based on the formulations of Pei 1992). The main degeneracy seen in the UV isochrone fitting involved metallicity. With all of the parameters allowed to be free, the metallicity of any cluster became unconstrained. Any change in metallicity could be accommodated by responsive changes in distance modulus and reddening. We therefore fixed the metallicity of the clusters to literature spectroscopic or photometric values, where available, and solar metallicity otherwise. For the most part, we ignored the RGB stars, since very few are detected in the NUV and those that are tend to be faint and dominated by a red leak. We do note below a few clusters, such as NGC 2477 (Section 3.4.24), where the RGB is prominent.

Other parameters, however, were easily constrained. The UV photometry proved particularly adept at measuring foreground reddening. Due to the differing orientations of the reddening vector—mostly blueward in the $uvm2-uvw1$ diagram and faintward in the $uvw2-uvw1$ diagram—an incorrect reddening produces a discrepancy in the location of the MS for a given distance modulus. With too much reddening, for example, the $uvm2-uvw1$ isochrone tends to end up above the MS, while the $uvw2-uvw1$ isochrone tends to end up below (Figure 2). Only the correct reddening value allows both isochrones to line up with the MS. This allowed age and distance modulus to be varied independently to match the MSTO. We are therefore confident in our measures of foreground reddening, age, and distance given the assumed metallicity.

Most of our program clusters were deliberately chosen to have low foreground reddening, which precluded any analysis of the reddening law itself (set, by default, to the Milky Way reddening law). However, for a few clusters, we were able to explore this issue to a modest extent (see, e.g., Collinder 220; Section 3.4.40)

As cataloged in Table 2 and in the notes on individual clusters, the isochrones performed very well. In most cases, we found that the photometry was consistent with the predictions of theoretical isochrones set to literature values. For a number of clusters, however, we had to substantially revise the parameters to produce consistent fits. This was particularly common among third-quadrant clusters in which the literature values sometimes described the foreground/background disk sequence, rather than the cluster. In this region of the sky, the reddening along the line of sight causes the "blue wall" of disk MSTO stars to veer redward as it gets fainter, making it resemble an MS. However, applying the *Gaia* astrometric membership (as well as radial velocity memberships, when available) made it clear that this was not the cluster sequence, which was well-defined in the *Gaia* astrometry.

Notes on the individual clusters are detailed below in order of ascending R.A. Because this is a large survey program, we do not go into great detail on our program clusters, many of which are worthy of a paper of their own. However, we do comment on discrepancies between our derived values and those found in the literature, the presence of unusual stellar

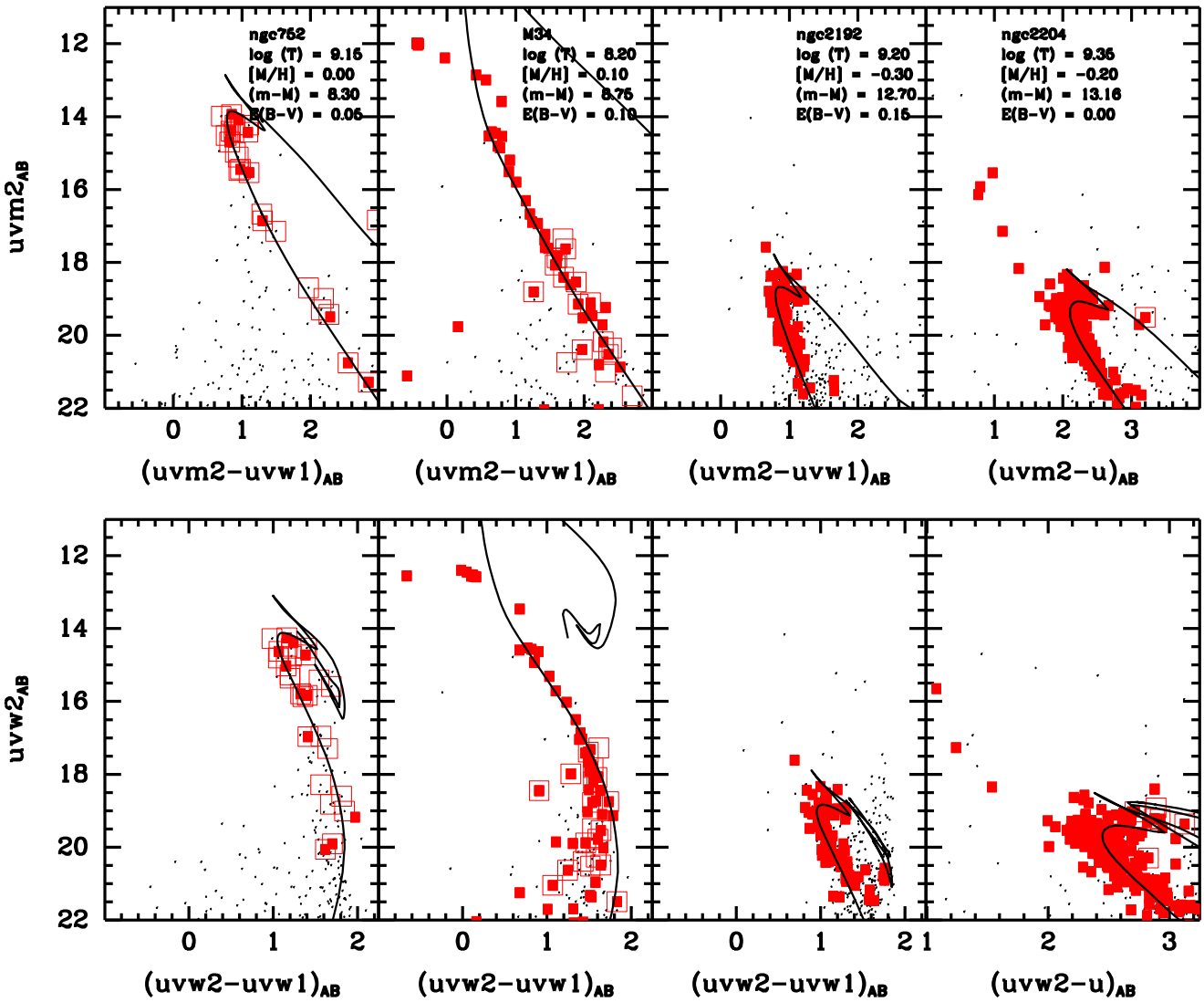

Figure 3. The CMDs of the open clusters NGC 752, M34, NGC 2192, and NGC 2204 (left to right). The solid lines are PARSEC-COLIBRI isochrones set to the parameters in the text. Filled red squares show astrometric members selected from *Gaia* DR2 by CG18, while open squares are spectroscopic members from either MMU or sources given in the text.

types in any cluster, and any potential broadening in the MSTO.

3.4. Individual Clusters

3.4.1. NGC 752

Situated well below the Galactic midplane in the second Galactic quadrant, NGC 752 is very well-studied, with several cluster members established as photometric standards and numerous thorough photometric and spectroscopic surveys in the literature. Its age (1.4 Gyr), detailed abundance ratios, and projected orbit make NGC 752 a typical representative of the family of old disk clusters (Carraro & Chiosi 1994; Maderak et al. 2013; Böcek Topcu et al. 2015; Twarog et al. 2015). Its similarity to disk red giants is evidence that much of the disk population formed from disrupted clusters (Reddy et al. 2012a, 2012b).

The UVOT field only encloses the central regions of this dispersed cluster (K13 measured a radius of 1°.4 but a core radius of 3′.0). However, the *Gaia* DR2 membership selection shows a clear MS (Figure 3, first column). We cross-identify numerous spectroscopic members cataloged by Daniel et al. (1994), all of which lie within the CG18 selection. The NGC 752 member stars align almost perfectly with the isochrone predicted by the parameters given in Twarog et al. (2015), which is expected given how well-studied and cataloged this cluster is.

3.4.2. M34

A second-quadrant cluster situated well below the Galactic midplane, M34 has been extensively studied and shown to be a solar or slightly supersolar abundance intermediate-age (200 Myr) moderately reddened ($E(B-V) \sim 0.10$) cluster (Jones & Prosser 1996; Schuler et al. 2003). An outer radius of 43′.8 was measured by K13, indicating that M34 fills the entire UVOT field, and we are only able to image the central regions of the cluster (K13 measured a core radius of 9′.6).

The *Gaia* astrometry shows a clean separation from the field that contains the spectroscopic members listed by Meibom et al. (2011) and traces a clear MS (Figure 3, second column). Comparison to the M17 isochrones yields a distance and reddening consistent with previous studies. We cannot

constrain the age of the cluster, as the upper MS is saturated on the UVOT exposures. However, we can apply a lower limit to the age of 320 Myr, given the extent of the MS we detect. We also show a number of cluster member stars blueward of the primary sequence. These stars could represent the top of a faint white dwarf sequence.

The lower end of the MS differs from the isochrones in the ($uvw2 - uvw1$) CMD (lower panel). As shall be seen, this discrepancy is common in clusters that are close enough for UVOT to probe the lower MS. We should note that this is near the point at which the red leak begins to take over the isochrones, as these stars are too cool ($T_{\rm eff} < 6300$ K) to produce significant UV light. Indeed, the only way to make the isochrone match the data on the lower MS is to significantly increase the reddening (which causes the isochrones to miss the upper MS in both panels). As the reddening increases, these faint stars become "bluer" because the red leak flux in the *uvw*1 band is extinguished faster than the red leak flux in the *uvw*2 band. Given the known issues with fitting UV isochrones to faint red stars (Section 4), we elected with this cluster (and other clusters demonstrating similar issues) to be guided by the bright MS.

3.4.3. NGC 2192

Located above the Galactic midplane, NGC 2192 is a second-quadrant cluster. Photometry from Park & Lee (1999) and Tapia et al. (2010) indicate that it is old (1.3 Gyr) and metal-poor ([M/H] ~ -0.3), an assessment shared by the global surveys of Paunzen et al. (2010) and K16. It does not have a previous spectroscopic survey.

The astrometric selection results in a clear MS in both CMDs (Figure 3, third column). We find that the cluster is well fit by the parameters derived by previous investigators with a slightly older age of 1.6 Gyr, assuming the photometric metallicity of [M/H] $= -0.3$. We identify one potential member star that is brighter and bluer than the nominal MSTO. This star is identified as a 100% likely member by CG18 and could represent a blue straggler. The MSTO of NGC 2192 does show some broadening beyond what would be expected from photometric errors alone. That may indicate that NGC 2192 has an eMSTO, although it is a bit at the older range for clusters that would have potential eMSTOs. It could also represent either photometric scatter in an old faint cluster or differential reddening in a moderately reddened cluster. Our analysis shows that differential reddening of even 0.05 mag would be enough to create the relevant scatter given the high sensitivity of the NUV filters to reddening. However, there are not enough bright stars in NGC 2192 to measure any spatial variation. Spectroscopic study could resolve this issue.

3.4.4. NGC 2204

Situated 16° below the Galactic plane in the third quadrant, NGC 2204 is a slightly metal-poor ([M/H] $= -0.20$), old (1.6 Gyr) cluster (Kassis et al. 1997; Jacobson et al. 2011). While it has been surveyed spectroscopically, these surveys have focused on old red giant stars, most of which are faint in the UV. Our data do not include the *uvw*1 passband but do include the redder *u* passband.

The fourth column of Figure 3 shows the CMDs compared to the M17 isochrones. The astrometric selection overlaps the member stars from the radial velocity surveys. Selecting stars as members based on either astrometry or radial velocity reveals a clear sequence of stars in the CMD. Our isochrone fits to the cluster favor a slightly older age (2.3 Gyr) than previous studies with minimal reddening (although slightly larger reddening with an SMC-like extinction law would also be consistent with the data). Note that NGC 2204 has a prominent population of blue stragglers, which are all confirmed as astrometric members. This confirms the detection of BSSs by Frogel & Twarog (1983).

3.4.5. NGC 2243

Located well below the Galactic midplane, NGC 2243 is a third-quadrant cluster. Previous studies by Twarog et al. (1997) and Jacobson et al. (2011) have found it to be old (5 Gyr) and metal-poor ([M/H] $= -0.42$). The radial velocity survey of MMU only measured two member stars, both of which are faint RGB stars that do not have UVOT counterparts.

Stars selected from CG18 form clean sequences in the CMDs (Figure 4, first column) that are well fit by the M17 isochrones with parameters similar to previous studies, with slightly lower metallicity ([M/H] $= -0.5$) and minimal reddening. We also identify a number of BSSs that are astrometric members.

3.4.6. NGC 2251

Located near the Galactic midplane, NGC 2251 is a third-quadrant cluster. Parisi et al. (2005) and Reddy et al. (2013) studied the cluster, revealing it to be slightly metal-poor ([M/H] $= -0.1$) and of intermediate age (300 Myr) with moderate reddening ($E(B-V) = 0.20$).

The astrometric selection includes one spectroscopic member from MMU. The member stars show a clear CMD sequence that corresponds almost exactly to the consensus literature values, with slightly higher reddening ($E(B-V) = 0.25$) and age (Figure 4, second column). We do note that the MSTO is near the saturation limit, but we do not find a large number of saturated stars in the image, so it is likely that this represents the true MSTO and thus the true age of the cluster.

3.4.7. NGC 2281

Positioned 16° above the Galactic midplane, NGC 2281 is in the third quadrant. Studies by Glaspey (1987) and Netopil (2017) indicate that it is of intermediate age (600 Myr) and solar metallicity. It is also one of the few clusters to have been previously studied in the UV using FUV data from *GALEX* (Smith 2018). The latter study found that the two-color FUV-optical sequence of NGC 2281 was slightly offset from that of the Hyades and Coma Ber, suggesting that it was younger than those two comparison clusters. However, this conclusion was tentative given the uncertainty in reddening. A radius of 24.′3 was measured by K13, so the UVOT images only cover the center of this low-density cluster.

The astrometric membership includes one spectroscopic member from MMU and defines a clear sequence in the CMDs (Figure 4, third column) that corresponds almost exactly to the consensus literature values, with slightly higher reddening ($E(B-V) = 0.15$). That the reddening is slightly higher than the value assumed in Smith (2018) would allow NGC 2281's two-color sequence to better overlap that of the Hyades and Coma Ber (see their Figure 5, which assumes $E(B-V) = 0.06$).

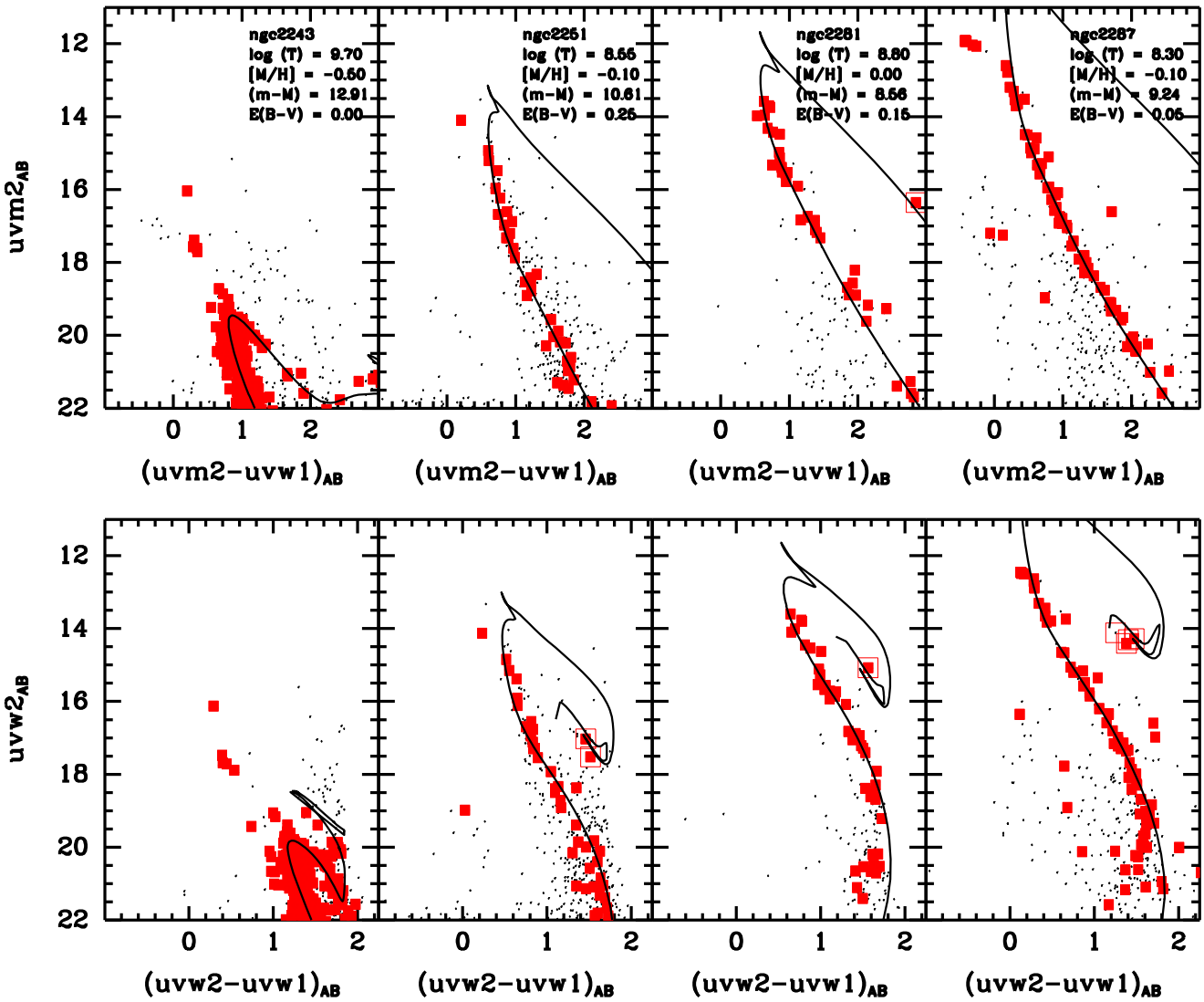

Figure 4. The CMDs of the open clusters NGC 2243, NGC 2251, NGC 2281, and NGC 2287 (left to right). The solid lines are PARSEC-COLIBRI isochrones set to the parameters in the text. Filled red squares show astrometric members selected from *Gaia* DR2 by CG18, while open squares are spectroscopic members from either MMU or sources given in the text.

This would be consistent with our estimate of an NGC 2281 age similar to that of the Hyades and Coma Ber.

3.4.8. M41 (NGC 2287)

Situated below the Galactic midplane, NGC 2287 (M41) is a bright nearby second-quadrant cluster. Extensive study has shown it to be young (200 Myr), minimally reddened, and with a high binary fraction (Harris et al. 1993; Dobbie et al. 2012). The UVOT field only covers the central region of the cluster (K13 measure a radius of 26.′4), and the data suffered from massive saturation from its many bright stars, which prevented both adequate PSF fitting and photometry of some of the brightest cluster members. It also created numerous false detections around the image artifacts, but these were easily removed by matching to the *Gaia* DR2 catalog.

The astrometric selection includes a number of radial velocity members from MMU. Selecting these stars and examining their aperture photometry shows a clear narrow MS that is well fit by the M17 isochrones with parameters similar to those derived by previous investigators (Figure 4, fourth column). The saturation limits our analysis, allowing us to only place an upper limit (500 Myr) on the age of M41 and making it impossible to confirm the eMSTO report by Cordoni et al. (2018). We detect a number of confirmed astrometric members along a probable white dwarf sequence and show the deviation in the ($uvw1 - uvw2$) colors seen in several other clusters.

3.4.9. NGC 2301

Located within the Galactic midplane, NGC 2301 is a bright third-quadrant cluster. The catalogs of K16 and Paunzen et al. (2010) describe it as slightly metal-rich ([M/H] = +0.06) and with a small amount of foreground reddening ($E(B-V) = 0.06$). It has been extensively studied for variable stars (see, e.g., Wang et al. 2015). As with NGC 2287, which it bears a striking similarity to, there is a plethora of bright saturated stars that prevented PSF fitting photometry. The data presented are aperture photometry cleaned by matching to *Gaia* DR2 and corrected to the same aperture as the PSF photometry.

The astrometrically selected CMD (Figure 5, first column) shows clear loci for the cluster stars. The one member star cataloged by MMU is well within the proper-motion locus and

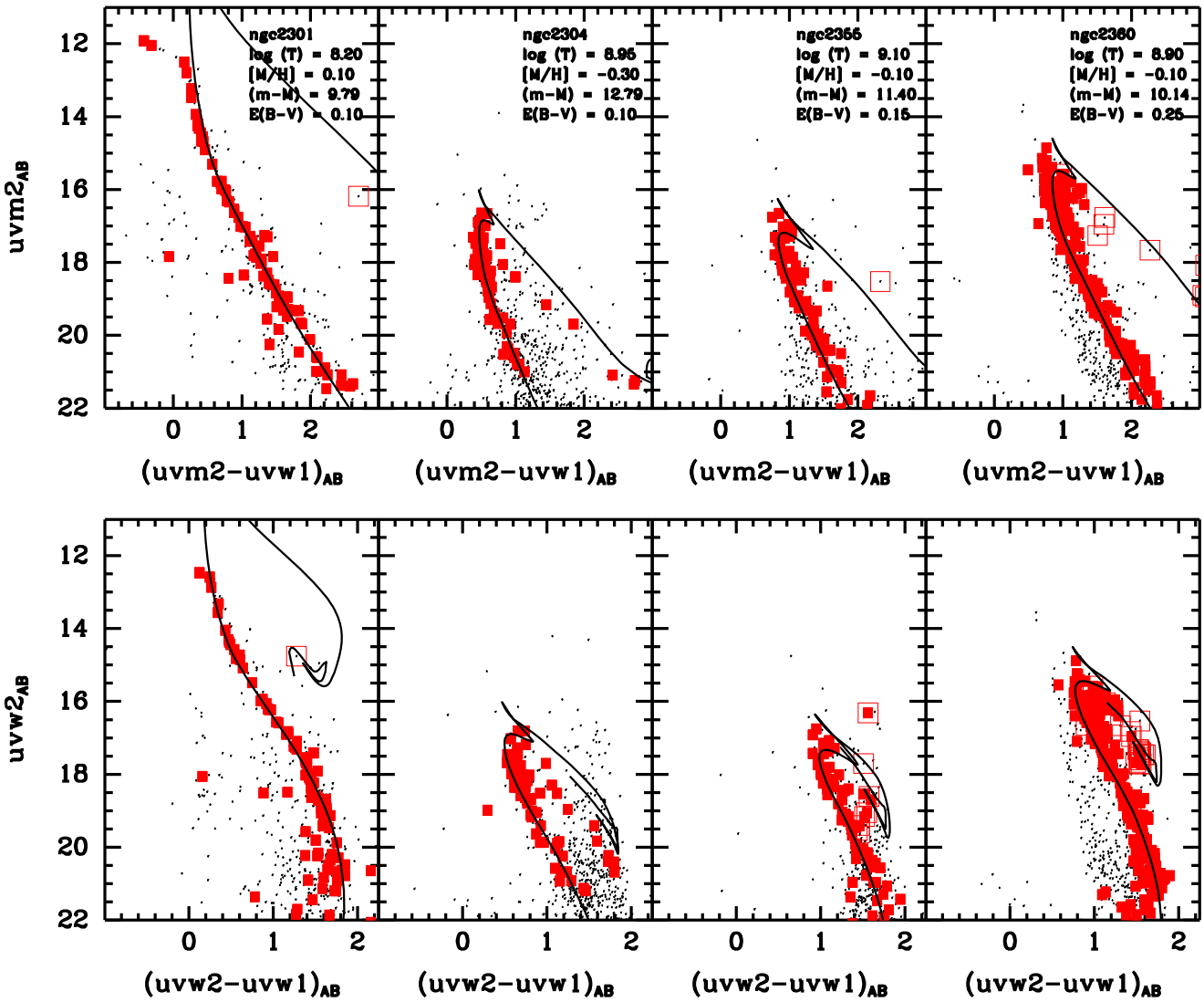

Figure 5. The CMDs of the open clusters NGC 2301, NGC 2304, NGC 2355, and NGC 2360 (left to right). The solid lines are PARSEC-COLIBRI isochrones set to the parameters in the text. Filled red squares show astrometric members selected from *Gaia* DR2 by CG18, while open squares are spectroscopic members from either MMU or sources given in the text.

along the RGB, albeit significantly fainter than expected. The M17 isochrones fit the photometry quite well, providing an upper limit on the age of 400 Myr and favoring a slightly higher foreground reddening ($E(B-V) = 0.10$).

3.4.10. NGC 2304

Located above the Galactic midplane, NGC 2304 is a third-quadrant cluster. Multiple photometric studies have been done, producing a broad range of parameters, as shown in Table 2 (Ann et al. 2002; Hasegawa et al. 2008; Lata et al. 2010; Oralhan et al. 2015). We were unable to identify a comprehensive radial velocity catalog, and the cluster was not surveyed by MMU.

The astrometric selection produces a clean CMD (Figure 5, second column). The M17 isochrones favor a cluster that is of intermediate age (900 Myr), moderately metal-poor ([M/H] = −0.3), and slightly reddened ($E(B-V) = 0.10$). Interestingly, our fit is slightly improved if we use an SMC reddening law (with no blue bump) as opposed to a Milky Way reddening law, although the difference is very small at such a low level of foreground reddening.

3.4.11. NGC 2343

Situated near the Galactic midplane, NGC 2343 is a third-quadrant cluster. Peña & Martínez (2014) showed the cluster to be young (12 Myr) and metal-poor, with [Fe/H] ∼ −0.4 based on $uvby - \beta$ photometry. It would be unusual for such a young cluster to be so metal-poor. Netopil et al. (2016), by contrast, estimated a photometric metallicity if [Fe/H] = −0.03. Several catalogs, including WEBDA, list the cluster at [Fe/H] = −0.3, but these all appear to trace back to a photometric metallicity estimate of [Fe/H] = −0.2 from Claria (1985).

The CG18 catalog of NGC 2343 was among a few third-quadrant clusters that had very few stars with high cluster membership probabilities. We therefore created our own membership probability measures by fitting two Gaussians to the distribution of proper motions in R.A.–decl. space. Cluster membership was defined as the ratio of the two Gaussians, and members with ratios greater than 9.0 were identified as likely members. This method was initially applied to all of our program clusters. For most, it produced member catalogs almost identical to CG18. We utilized the CG18 membership,

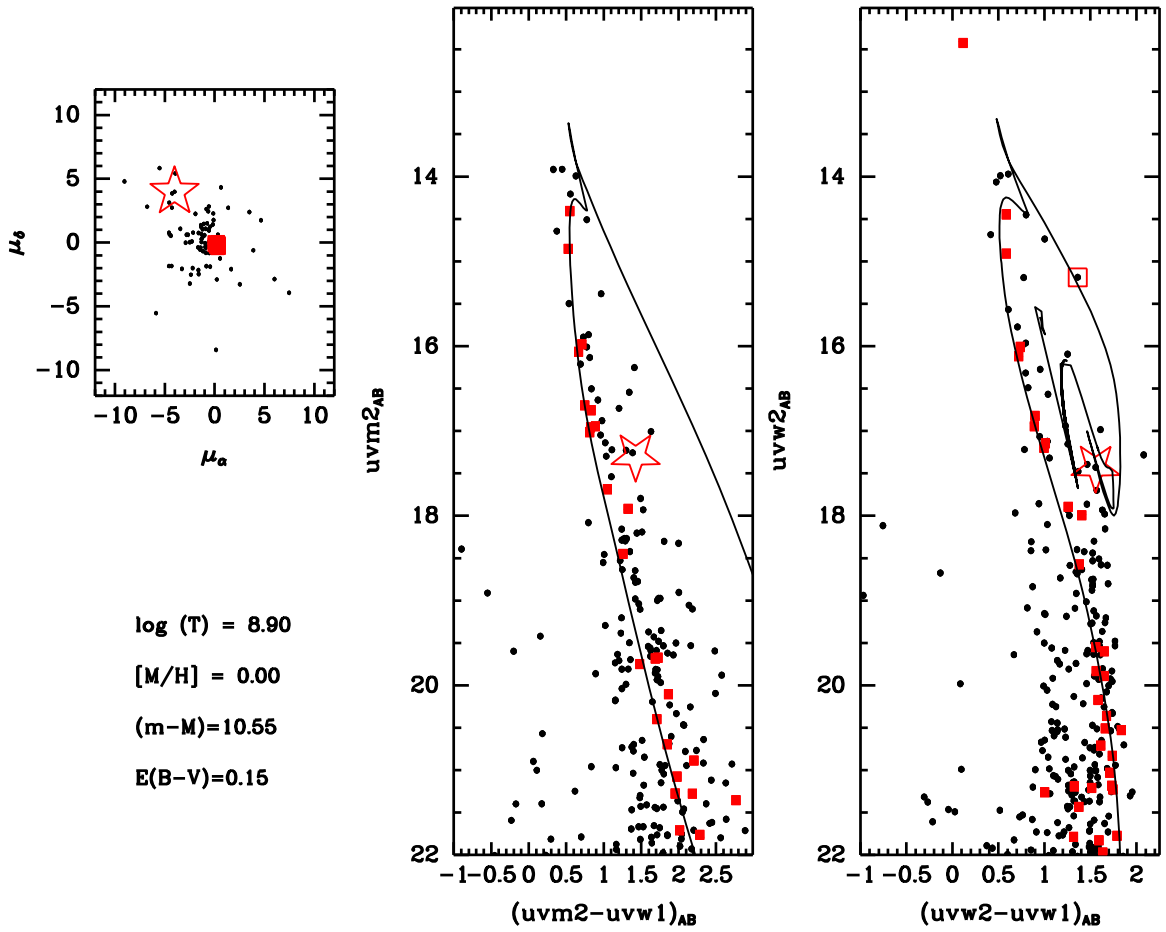

Figure 6. The VPD and CMDs of the cluster NGC 2343 compared to the best-fit isochrones of PARSEC-COLIBRI. The brightest stars in the cluster are saturated, preventing us from measuring more than an upper limit on the age of the cluster. The filled red squares show astrometric members selected from *Gaia* DR2, while the open red square is a spectroscopic member from MMU. The open stars mark the star used by Peña & Martínez (2014) to estimate the metallicity of the cluster.

as it included more dynamical information and its membership lists were slightly more conservative. The cluster NGC 2343 was one of the few where the methods disagreed.

Figure 6 shows the VPD of the cluster and a tight clump of stars toward the edge of the field star distribution. Using these as cluster members, we find the metallicity estimate of Peña & Martínez (2014) is likely in error. The star they identify as 29 and use as their metallicity estimator is almost certainly not a member of the cluster, being placed well to the edge of the field star distribution and off of the MS. It is most likely a metal-poor thick disk or halo star. In the UVOT images, HD 54387, used as the metallicity estimator by Claria (1985), is saturated. Its proper motion does place it near the NGC 2343 proper motion, however.

The member stars trace a clear MS. Given the uncertainty in the metallicity, we adopt solar metallicity. If the cluster is indeed slightly metal-poor, the result would be a shorter distance modulus ($m-M=9.64$). While our photometry is limited in its ability to measure the age of this cluster, and we can only give an upper limit (the bright star seen in the $uvw2-uvw1$ CMD is saturated), we find it unlikely that NGC 2343 is a very young cluster, given the small number of bright saturated stars in the images and the location of the spectroscopically confirmed RGB star from MMU. The location of the RGB star, approximately 3 mag brighter than the MS, is consistent with an intermediate-age population. A young population would have a much hotter and brighter RGB sequence. It is therefore likely that the cluster age is more in the range of 100–500 Myr, as indicated by our photometry and Netopil et al., than the 12 Myr measured by Peña & Martínez.

3.4.12. NGC 2355

Located above the Galactic midplane, NGC 2355 is a third-quadrant cluster. Previous investigations have revealed it to be slightly metal-poor ([M/H] = −0.06) and of intermediate age (900 Myr; Donati et al. 2015) with typical disk abundance ratios (Jacobson et al. 2011).

The CMDs (Figure 5, third column) show a fit consistent with previous investigations but favoring a slightly higher age of 1.1 Gyr. The MSTO of the cluster proved difficult to fit precisely with any combination of parameters. Notably, we find that there is some broadening in the MSTO. This could indicate an eMSTO but could also be the effect of differential reddening (to which the NUV is particularly sensitive at the level of $E(B-V)=0.05$). The cluster may be worthy of future spectroscopic study to determine the nature of the MSTO broadening.

3.4.13. NGC 2360

Located above the Galactic midplane, NGC 2360 is a third-quadrant cluster. The literature on this cluster contains widely different values for the parameters, as shown in Table 2. Reddy et al. (2012a) and Sales Silva et al. (2014) favored a large distance ($m-M=11.72$) and young age (560 Myr), while

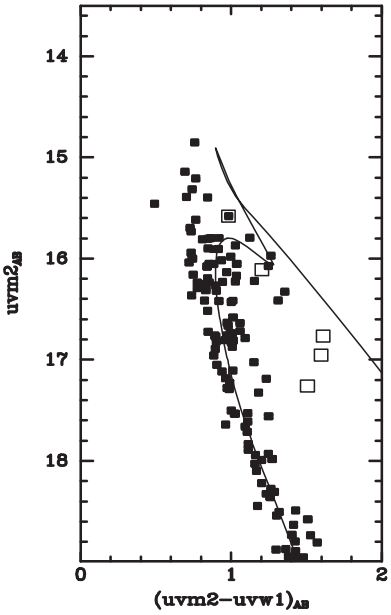

Figure 7. Close-up of the MSTO region of NGC 2360. The panel shows *Gaia*- and spectroscopically selected members. The MSTO region is very broad due to the combination of eMSTO, convective hook, and the beginning of the RGB.

Clariá et al. (2008) favored a closer distance ($m - M = 10.09$) and older age (1.8 Gyr). This discrepancy is likely due to the presence of two distinct color–magnitude sequences in the field, something we have observed in numerous low-latitude third-quadrant clusters, as detailed in a number of following clusters. One of these represents the foreground disk, the other the cluster itself. WEBDA lists the cluster at the longer distance and younger age.

Previous spectroscopic studies have been mostly focused on red giants, which our data cannot use to constrain the properties of the cluster due to their lack of UV emission. However, the astrometric selection (Figure 5, fourth column) clearly aligns with the brighter/redder MS. This sequence is favored independently by the proper motions, parallaxes, and spatial distribution. Fitting the M17 isochrones to this sequence produces a fit consistent with the Claria et al. result and inconsistent with the Reddy/Sales Silva result currently listed in WEBDA. We conclude that the closer/older solution is likely the correct one.

The cluster NGC 2360 is one of the few in our sample that is both bright enough and close enough to explore the fine structure of the MSTO. Cordoni et al. (2018) identified it as a cluster with an eMSTO. This region of the CMD is tricky because it overlaps both the convective hook in the MSTO and the beginning of the RGB. However, the $uvm2 - uvw1$ diagram shows that the MSTO is broader and more structured than one would expect from a simple stellar population (the fit isochrone splits the difference between the blue and red edges of the MSTO). Figure 7 shows a close-up of this turnoff region, and it appears to confirm the Cordoni et al. (2018) discovery, hinting at a bifurcation in the MSTO, likely as a result of variation in stellar rotation.

3.4.14. Berkeley 37

Berkeley 37 is a faint third-quadrant cluster situated above the plane. The only photometric study to date is that of Oralhan et al. (2015), who showed it to be distant ($m - M = 13.60$) with light extinction ($E(B - V) = 0.05$) and an intermediate age (600 Myr). A slightly shorter distance with more reddening was derived by K16.

The CG18 selection did not pick out many cluster members, likely due to the similarity of the cluster kinematics to that of the disk. We applied our own selection criteria using the double Gaussian method described for NGC 2343 (Section 3.4.11). The VPD shows a tight clump of stars within the dense field star distribution. This clump corresponds to a faint intermediate-age MS in the CMD (Figure 8, first column). We measure cluster parameters similar to those of Oralhan. Our membership survey includes two stars that could be potential blue stragglers. One of these is in the core of the cluster, while the other is in the outskirts. This indicates that the former is likely a genuine blue straggler, while the latter may be a field star contaminant for a cluster in a very dense region of the sky.

3.4.15. NGC 2374

Situated near the Galactic midplane, NGC 2374 is third-quadrant cluster. It has been poorly studied, with no spectroscopic metallicity available. The only recent photometric study is that of Carraro et al. (2015), who found it be young (250 Myr) and argued that its position near the Galactic warp makes it consistent with either a thick disk cluster or an extended thin disk cluster.

Only one member star was identified by MMU: a red giant that is faint and well removed from the MS. Only a handful of astrometric members were identified by CG18. The VPD, however, shows a clear clump of stars well removed from the disk sequence that defines narrow photometric sequences in the CMDs (Figure 8, second column). We derive parameters similar to those of Carraro et al. (2015), albeit at slightly higher reddening ($E(B - V) = 0.15$). Like many third-quadrant clusters, we also see the "second sequence" of the disk.

3.4.16. NGC 2396

Positioned just above the Galactic midplane, NGC 2396 is a third-quadrant cluster. It has never been the focus of an individual study, and the only parameters in the literature come from the comprehensive survey of K16, who showed the cluster to be nearby ($m - M = 8.68$), of intermediate age (300 Myr), and minimally reddened ($E(B - V) = 0.05$).

The CG18 astrometric selection produces a clear sequence in CMDs (Figure 8, third column). However, the MS is over 2.5 mag fainter than that predicted by the K16 parameters. The best fit shows a similar age (250 Myr), slightly more reddening ($E(B - V) = 0.15$), and a dramatically larger distance ($m - M = 11.12$). Interestingly, the faint end of the $uvw2 - uvw1$ sequence does not show the deviation between data and isochrone that other bright clusters show, even though the underlying parameters of the stellar population are similar.

3.4.17. NGC 2420

Positioned 19° above the Galactic midplane, NGC 2420 is a third-quadrant cluster. Extensive investigation (von Hippel & Gilmore 2000; Anthony-Twarog et al. 2006; Souto et al. 2016) has revealed it to be old (2 Gyr) and slightly metal-poor ([Fe/H] ~ -0.14). It is also one of the few clusters to be extensively studied in the UV by *GALEX* (De Martino et al. 2008) and has extensive radial velocity data in MMU.

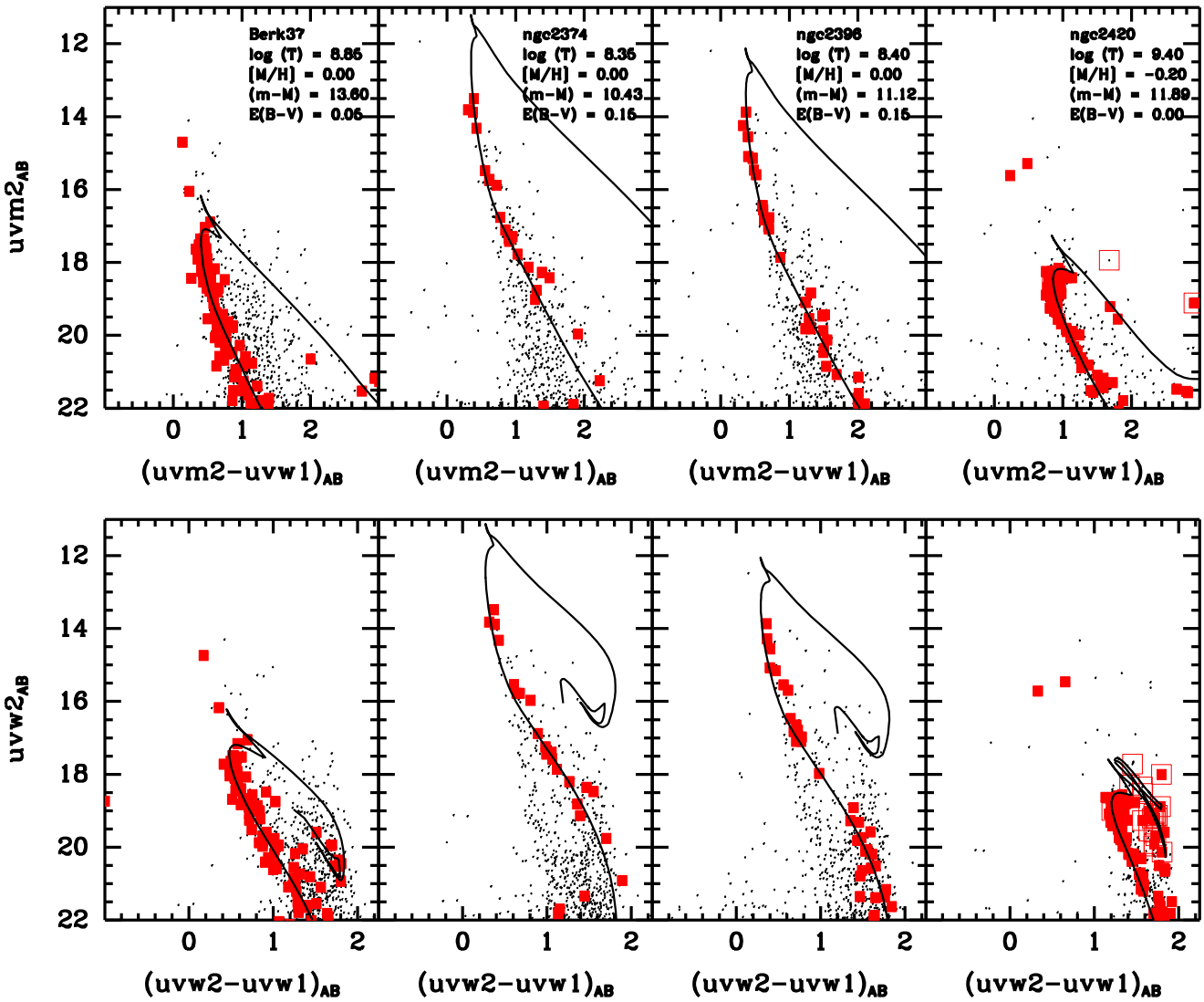

Figure 8. The CMDs of the open clusters Berkeley 37, NGC 2374, NGC 2396, and NGC 2420 (left to right). The solid lines are PARSEC-COLIBRI isochrones set to the parameters in the text. Filled red squares show astrometric members selected from *Gaia* DR2 by CG18, while open squares are spectroscopic members from either MMU or sources given in the text.

Fitting the M17 isochrones to the astrometrically selected stars using literature values (Figure 8, fourth column) produces a reasonable fit but with a slight discrepancy: the $uvm2 - uvw1$ model colors are a little too red, and the $uvw2 - uvw1$ colors are a little too blue. A detailed examination of the photometry, including a direct comparison to the standard *Swift*/UVOT pipeline photometry produced by UVOTSOURCE, shows no error in the photometry. The cluster gives no indication of any chemical abundance anomalies, showing typical metal-rich disk abundances with solar-type α-abundances (Souto et al. 2016). Lowering the metallicity to $[Fe/H] = -0.3$ and decreasing the cluster distance produces very good isochrone fits. However, the abundance of NGC 2420 is very well established through multiple spectroscopic studies. Previous research has indicated some variation in the UV reddening law within external galaxies and within the Galaxy, particularly the R_V value and bump strength (Siegel et al. 2014; Hagen et al. 2017), but the foreground reddening in NGC 2420 is low, and modifying the reddening law produces only minor changes. At this point, we are unable to explain the slight discrepancy in NGC 2420 compared to other clusters that have better fits.

We do note, however, that the MSTO does show a bit of broadening, which would be consistent with an eMSTO. The cluster's 2 Gyr age is toward the lower end of the range where an eMSTO is expected to manifest before magnetic braking evens out the stellar rotation rates (Georgy et al. 2019). It would be worth further investigation to determine if the MSTO stars show differences in rotation rates and potentially set the age limits of the eMSTO phenomenon on a more empirical footing.

3.4.18. NGC 2422

Positioned near the Galactic midplane, NGC 2422 is a bright nearby third-quadrant cluster. Studies by Rojo Arellano et al. (1997) and Prisinzano et al. (2003) showed it to be very young (80 Myr) with moderate foreground reddening ($E(B-V) = 0.09$). Conrad et al. (2014) measured it as slightly metal-poor ($[Fe/H] = -0.03$) but within the uncertainties of solar metallicity. The cluster proved difficult to study due to the large number of saturated stars and the concomitant number of false detections in the diffraction spikes. The sample studied was only of stars that could be matched to *Gaia* DR2. The

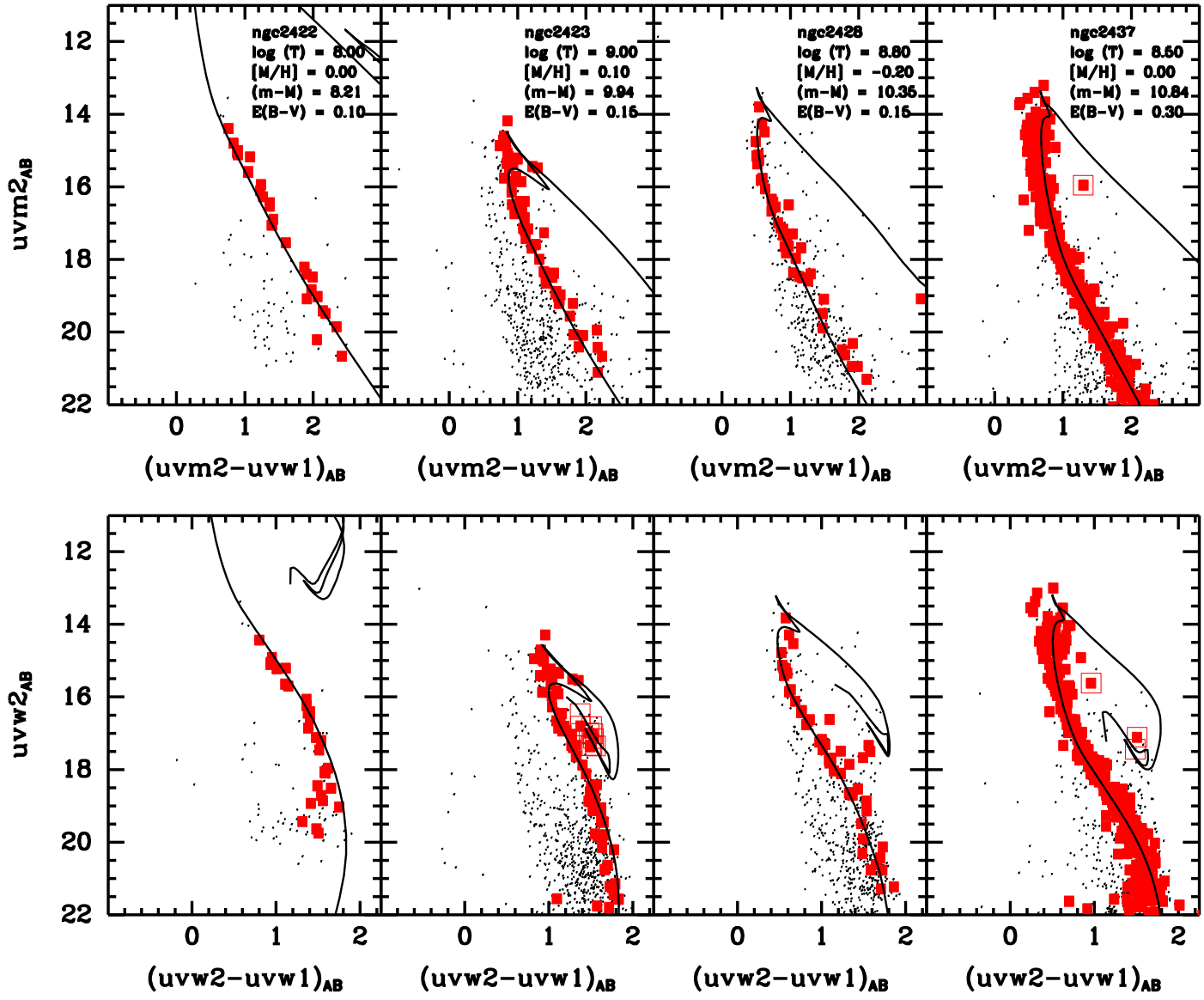

Figure 9. The CMDs of the open clusters NGC 2422, NGC 2423, NGC 2428, and NGC 2437 (left to right). The solid lines are PARSEC-COLIBRI isochrones set to the parameters in the text. Filled red squares show astrometric members selected from *Gaia* DR2 by CG18, while open squares are spectroscopic members from either MMU or sources given in the text.

cluster covers a large area of sky—37.′8 in radius according to K13—and thus we have only imaged the core.

The CMD (Figure 9, first column) shows a narrow young MS consistent with literature expectations. The brightest stars in the cluster are badly saturated, meaning we can only place an upper limit on the age. However, the reddening and distance are well constrained. As with other clusters, the faint end of the $uvm2 - uvw1$ sequence shows a deviation from the isochrone, bending more sharply toward the blue than predicted.

3.4.19. NGC 2423

Positioned above the Galactic midplane, NGC 2423 is a third-quadrant cluster. Prior study has revealed it be an intermediate-age (1 Gyr), metal-rich ([Fe/H] = +0.10) cluster (Clariá et al. 2008; Santos et al. 2009, 2012; Paunzen et al. 2010; Conrad et al. 2014).

Like NGC 2360 (Section 3.4.13), the CMD shows a double sequence of the old thin disk and cluster (Figure 9, second column). The astrometric selection picks the brighter sequence and contains the radial velocity members identified by MMU. The M17 isochrones produce a fit with parameters consistent with the literature.

3.4.20. NGC 2428

Positioned 16° below the Galactic midplane, NGC 2428 is a third-quadrant cluster. Conrad et al. (2014) showed the cluster to be slightly metal-poor ([Fe/H = −0.15) with modest reddening ($E(B-V) = 0.05$). The global survey of K16 lists a shorter distance with heavier foreground reddening.

As with NGC 2360 and NGC 2423, the CMD (Figure 9, third column) shows a double sequence, and the WEBDA parameters, taken from Conrad et al., appear to trace the bluer sequence. The member stars favor the redder sequence, and the M17 isochrones give a fit more consistent with that of K16 than Conrad et al., indicating that this is the cluster sequence.

3.4.21. NGC 2437

Davidge (2013) shows NGC 2437 (M46), a bright cluster in the third quadrant, to be near solar metallicity, of intermediate age (200 Myr), and moderately reddened. The Conrad et al. (2014) survey identifies it as very metal-poor, with an [M/H] of −0.75, albeit with a very high uncertainty. It would be unusual, however, for such a young cluster to be so metal-poor. A radius of 34′.2 was measured by K13, indicating that UVOT only images the core of the cluster.

The astrometric selection of CG18 includes the radial velocity members identified by MMU and traces a long, narrow MS in the CMDs (Figure 9, fourth column). As noted above, the UV CMDs are not very adept at measuring metallicity, and NGC 2437 is a case in point. The properties of the cluster are well constrained at both low and solar metallicity. At solar metallicity, we derive fits close to the parameters of Davidge (2013) and K16, with a slightly higher reddening ($E(B-V)=0.30$) and shorter distance ($m-M=10.84$). If the cluster were indeed as metal-poor as indicated in Conrad et al. (2014), an isochrone with a significantly shorter distance modulus ($m-M=9.96$) and dramatically higher reddening ($E\ (B-V)=0.35$) would also fit the data quite well. Given the high uncertainty in the latter measure and the lower likelihood that such a young cluster would be so metal-poor, we list NGC 2437's parameters in Table 2 as derived for the higher metallicity.

3.4.22. NGC 2447

Situated within the Galactic midplane, NGC 2447 is a third-quadrant cluster. Studies by Clariá et al. (2005), Santos et al. (2009, 2012), Conrad et al. (2014), and Reddy et al. (2015) describe it as having slightly subsolar metallicity ([Fe/H] = −0.10) and intermediate age (400 Myr). The K13 radius of 30′.0 indicates that we observe only the core of the cluster.

Like many other third-quadrant clusters, NGC 2447 shows two sequences in the CMD (Figure 10, first column). The astrometric selection, however, favors the bright sequence of young stars. The M17 isochrones fit this sequence with parameters very similar to the literature values.

3.4.23. Berkeley 39

Berkeley 39 is a third-quadrant cluster situated 10° above the Galactic midplane. Previous studies (Carraro et al. 1994, 1999; Kassis et al. 1997; Frinchaboy et al. 2006) have shown the cluster to be massive, old (5.5 Gyr), and moderately metal-poor ([Fe/H] = −0.20) The extensive spectroscopic survey of Bragaglia et al. (2012) identifies 30 radial velocity cluster members with very small star-to-star variations in abundance, consistent with a simple stellar population. Unfortunately, only a handful of their program stars have counterparts in the UVOT data due to their cool temperatures and subsequent low-UV emission.

Because the cluster is old, reddened, and distant, we only detect the very top of the MS in the $uvw2-uvw1$ CMD (Figure 10, second column) and do not detect it at all in the $uvm2-uvw1$ CMD (most likely due to the lack of a red leak in $uvm2$). We are unable to constrain its properties on so tenuous a basis. However, overlaying isochrones from the consensus literature shows a rough agreement. Moreover, we detect a number of likely cluster members that would be along a potential blue straggler sequence.

3.4.24. NGC 2477

Located below the Galactic midplane, NGC 2477 is a third-quadrant cluster. Extensive previous investigation has shown it to be of intermediate age (1 Gyr) with moderate ($E(B-V)=0.25$) reddening (Jeffery et al. 2016). Metallicity estimates range from [Fe/H] = +0.07 (Bragaglia et al. 2008) to −0.19 (Conrad et al. 2014). We have taken the metallicity at an intermediate value of −0.10. The cluster is large, with a K13 radius of 27′.0, indicating that we only observe the core.

The astrometric and spectroscopic selection identifies a clear MS in the CMDs (Figure 10, third column). The M17 isochrones produce a fit consistent with the previous literature. However, we note that the MS is fairly broad and that this breadth occurs along the entire observed MS. It is likely that this represents differential reddening, as NGC 2477 is one of the few clusters we have that has moderate foreground reddening ($E(B-V)=0.25$), and even small variations can produce noticeable breadth in the CMD. We note at least three stars that are likely blue stragglers.

As noted above, we mostly ignore the RGB stars in the clusters due to their faintness and the dominance of the red leak in their photometric measures. However, NGC 2477 is one of those that has a prominent RGB. It is also well-surveyed spectroscopically. One of the most noticeable aspects of its CMD is that the RGB stars tend to land significantly blueward of the isochrone prediction. This tendency of the isochrone to miss the few RGB stars can be seen in other clusters, but this the clearest example. This suggests that the isochrones are not reproducing the NUV properties of the RGB accurately. The reasons for this could be many, but the two most likely are that the atmospheric models do a poor job of predicting the intrinsically low UV flux for such cool objects (likely due to opacity issues at low temperatures) and that our accounting for the red leak is incorrect. Further NUV investigation of bright field RGB stars would provide a better constraint on both of these inputs of the theoretical isochrones.

3.4.25. ESO 123-26

ESO 123-26 is a fourth-quadrant cluster positioned well below the Galactic midplane. It has not been the subject of individual study, with the only parameter estimates coming from global surveys such as K13 and K16.

This cluster is not included in the CG18 compilation and so we applied the double Gaussian selection method used for NGC 2343 (Section 3.4.11). The VPD shows a loose clumping of stars toward the outside of the field star distribution which corresponds to a clear color–magnitude sequence (Figure 10, fourth column). The best-fit isochrone is close to the K16 parameters but with a longer distance ($m-M=10.20$) and a slightly older age (500 Myr). We caution however, that the proximity of this cluster may mean that its brightest members are saturated, so this age should be regarded as an upper limit.

3.4.26. NGC 2479

A recent photometric study by Piatti et al. (2010) revealed NGC 2479, above the Galactic midplane in the fourth quadrant, to be old (1 Gyr) and relatively distant ($m-M=11.00$) with minimal foreground reddening.

The cluster is also not included in the CG18 study, and we applied our own astrometric selection (see Section 3.4.11). The VPD reveals a tight clump of stars toward the edge of the field

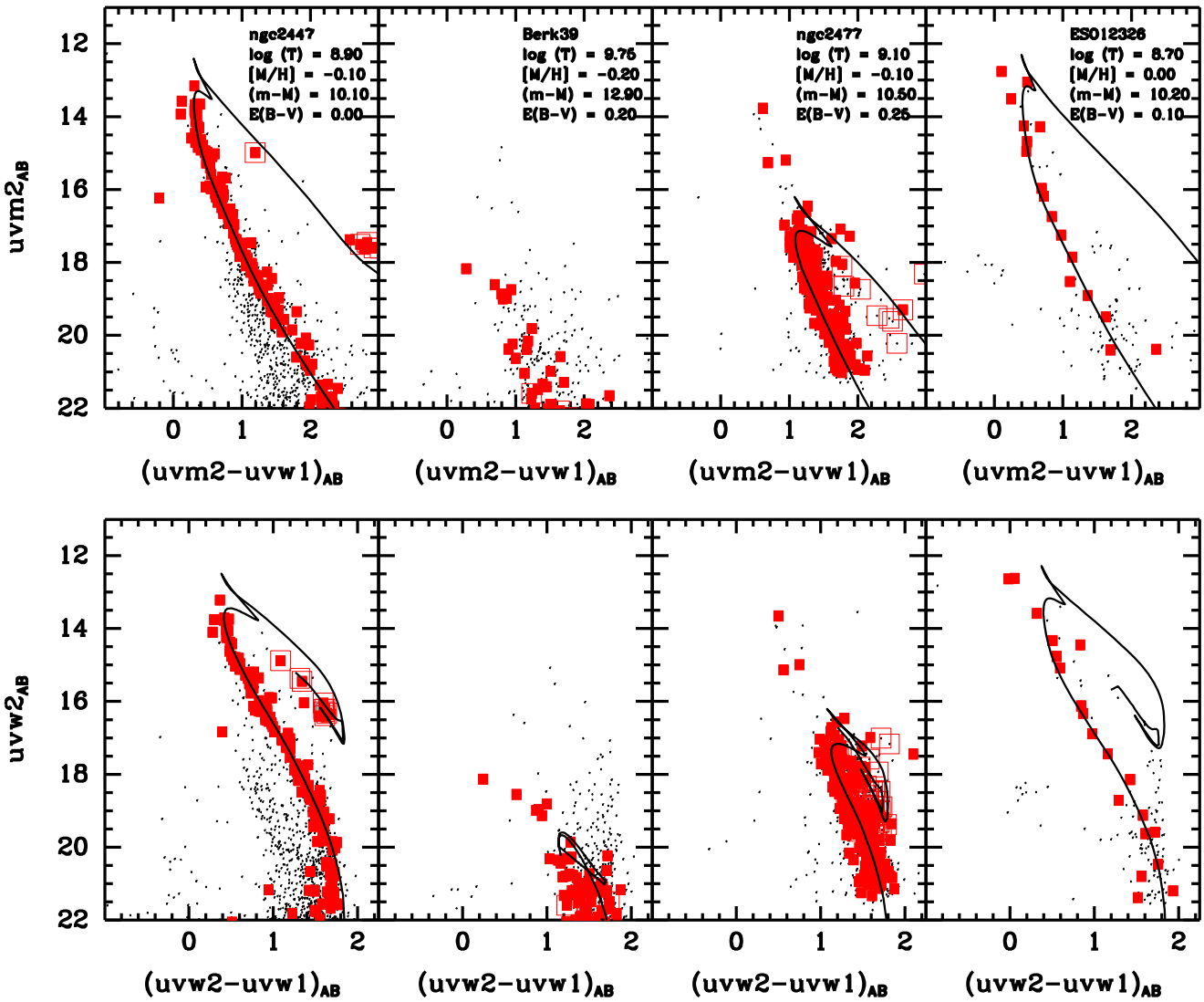

Figure 10. The CMDs of the open clusters NGC 2447, Berkely 39, NGC 2477, and ESO 123-26 (left to right). The solid lines are PARSEC-COLIBRI isochrones set to the parameters in the text. Filled red squares show astrometric members selected from *Gaia* DR2 by CG18, while open squares are spectroscopic members from either MMU or sources given in the text.

star distribution. Stars selected from this clump trace a narrow sequence in the CMD (Figure 11, first column). The parameters of Piatti et al. (2010) produce isochrones that overlay this sequence almost exactly with a slightly older age of 1.1 Gyr.

3.4.27. NGC 2482

Positioned just above the Galactic disk, NGC 2482 is a fourth-quadrant cluster. Recent studies have shown it to be an intermediate-age (400 Myr) near-solar metallicity cluster (Reddy et al. 2013; Conrad et al. 2014; Krisciunas et al. 2015). The astrometric selection shows a clear sequence in the CMD (Figure 11, second column). The M17 isochrones produce a fit similar to previous studies but with lower reddening ($E(B-V) = 0.05$).

3.4.28. NGC 2506

Located above the Galactic midplane, NGC 2506 is a third-quadrant cluster. Previous studies have shown it to be an old (2 Gyr) metal-poor ([Fe/H $= -0.3$) cluster (Lee et al. 2012; Reddy et al. 2012b; Anthony-Twarog et al. 2016). The cluster has also been the subject of extensive spectroscopic surveys that have confirmed its low metallicity (MMU; Anthony-Twarog et al. 2018).

The CMD shows a dominant locus of cluster stars that contains the radial velocity members of MMU and astrometrically selected members (Figure 11, third column). The M17 isochrones produce a fit consistent with prior literature given the assumed metallicity of [Fe/H] $= -0.3$. Also, NGC 2506 shows a very prominent blue straggler sequence, the brightest of which is both a proper-motion and radial velocity member. There is quite a bit of breadth to the MS, which is unexpected given the low reddening. The broadening occurs along the entire length of the MS rather than just the MSTO, making the nature of it unclear.

3.4.29. NGC 2509

Positioned above the Galactic disk, NGC 2509 is an older cluster. The literature shows a number of very different solutions to NGC 2509's properties. Sujatha & Babu (2003) argued for a very old age of 8 Gyr, while Tadross (2005) and Carraro & Costa (2007) found a more intermediate age of

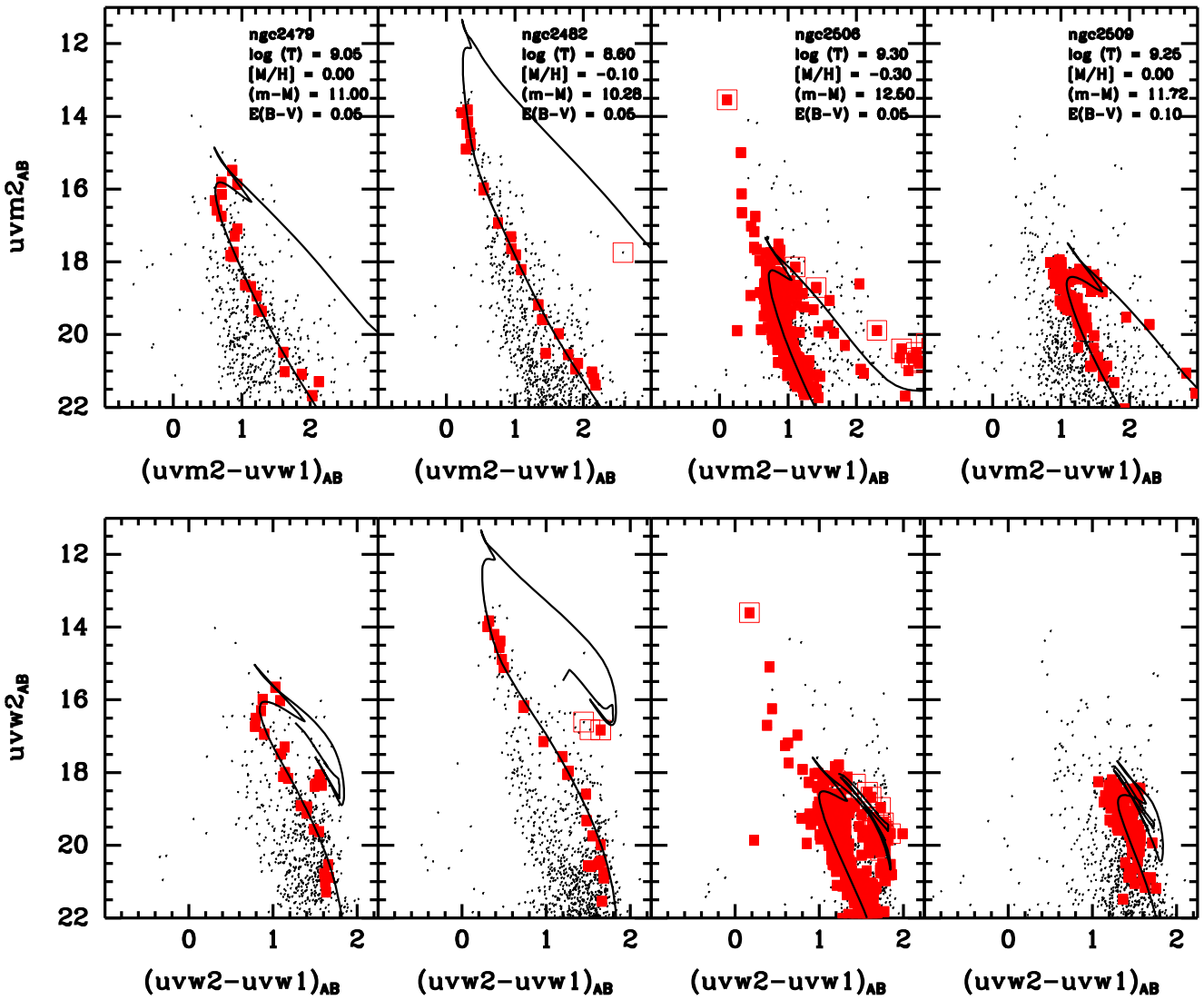

Figure 11. The CMDs of the open clusters NGC 2479, NGC 2482, NGC 2506, and NGC 2509 (left to right). The solid lines are PARSEC-COLIBRI isochrones set to the parameters in the text. Filled red squares show astrometric members selected from *Gaia* DR2 by CG18, while open squares are spectroscopic members from either MMU or sources given in the text.

1.2–1.6 Gyr but with a significant difference in distance modulus between them ($m - M = 11.50$ and 12.50, respectively). No spectroscopic metallicity is available, and those studies assumed solar metallicity.

The CG18-selected CMD (Figure 11, fourth column) shows a faint MS. Assuming solar metallicity, the best fit to the photometry is consistent with the Tadross et al. (2005) results, showing an older age (1.7 Gyr) and a shorter distance ($E(B - V) = 11.72$).

3.4.30. NGC 2527

Located near the Galactic midplane, NGC 2527 is a third-quadrant cluster. Reddy et al. (2013) found it be of intermediate age (450 Myr), slightly metal-poor ([Fe/H = −0.09), and slightly reddened ($E(B - V) = 0.04$), based on spectroscopy and photometry. Conrad et al. (2014) found it to be slightly more metal-rich ([Fe/H] = +0.06) but based only on two stars.

The CMD (Figure 12, first column) shows a clean sequence, well separated from the disk. We find parameters similar to those of Reddy et al. The age of the cluster is a bit uncertain, as the brightest MSTO stars are saturated. However, the curvature of the upper parts of the CMD is inconsistent with an age older than that found in Reddy et al. Note again that the *uvw*2 − *uvw*1 colors at the faint end of the MS are bluer than predicted by the isochrones.

3.4.31. NGC 2533

Positioned above the Galactic midplane, NGC 2533 is a third-quadrant cluster. The cluster has never been targeted for individual photometric study. However, basic parameters come from the blue straggler survey of Ahumada & Lapasset (2007) and the global survey of K16.

The CG18 selection showed very few member stars, so we applied our own proper-motion analysis, as detailed in Section 3.4.11. The CMD (Figure 12, second column) shows a rough faint MS and turnoff that are similar to the expectations from the K16 parameters. We adjusted those parameters slightly to a shorter distance ($m - M = 12.20$) and older age (700 Myr), although we emphasize that the analysis of this cluster is complicated by the somewhat high ($E(B - V) = 0.40$) reddening

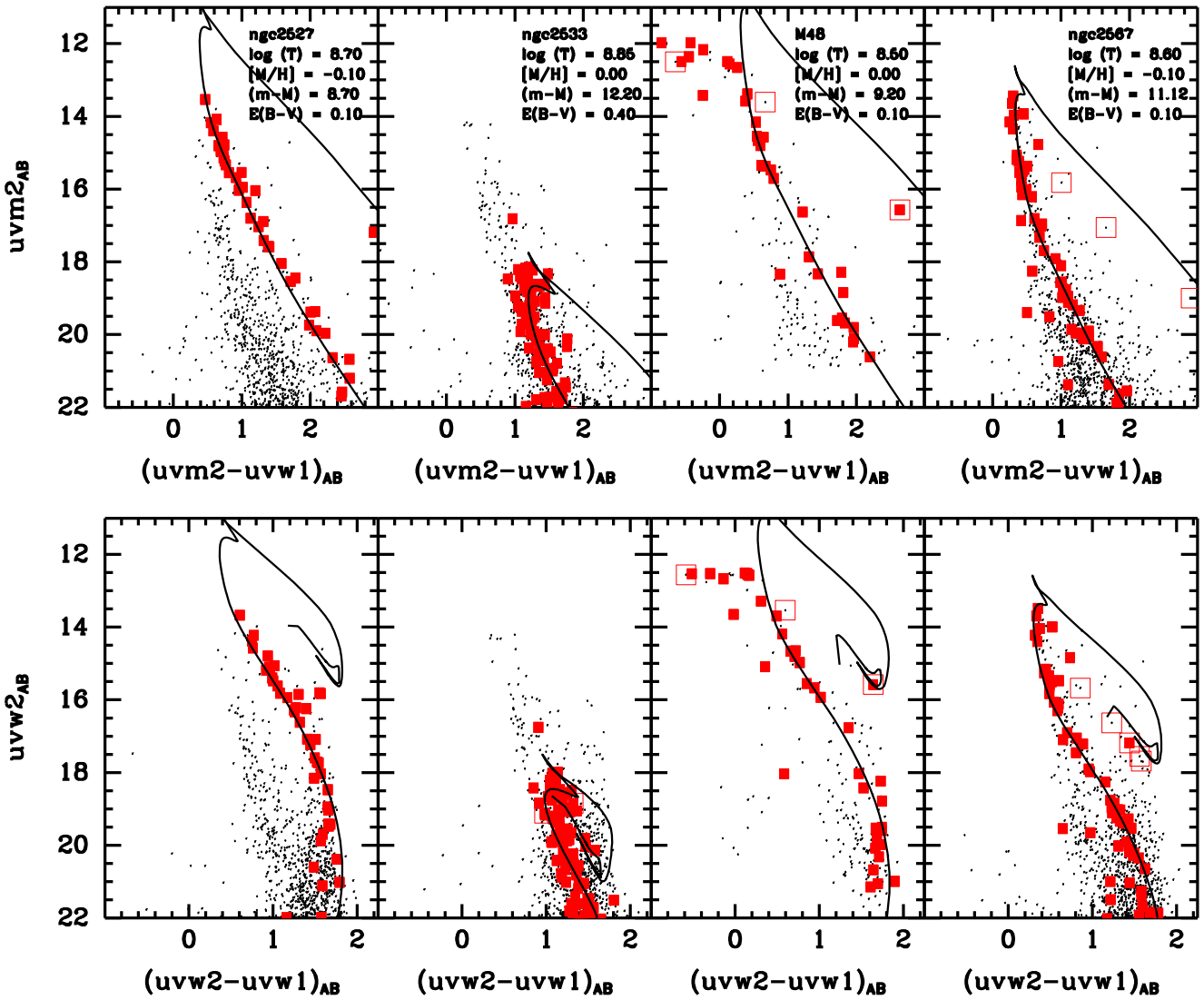

Figure 12. The CMDs of the open clusters NGC 2527, NGC 2533, M48, and NGC 2567 (left to right). The solid lines are PARSEC-COLIBRI isochrones set to the parameters in the text. Filled red squares show astrometric members selected from *Gaia* DR2 by CG18, while open squares are spectroscopic members from either MMU or sources given in the text.

and red leak causing the RGB to cross over the MSTO in the $uvw2 - uvw1$ CMD.

3.4.32. M48 (NGC 2548)

The cluster M48 is one of the most well-studied open clusters in the Galaxy. While the specific parameters of previous studies vary, there is a general consensus that it is close and of intermediate age (400 Myr), with minimal reddening (Rider et al. 2004; Balaguer-Núñez et al. 2005; Wu et al. 2005; Sharma et al. 2006). Most studies assume near-solar metallicity, although Balaguer-Núñez et al. measured a photometric metallicity of [Fe/H]–0.24. The massive size of the cluster (K13 measured a radius of 43′.2) indicates that we have only surveyed the central regions.

The field contains many saturated stars, so only stars with *Gaia* DR2 counterparts are shown in the CMD (Figure 12). Assuming solar metallicity, we derive similar parameters to the consensus literature, with slightly elevated reddening ($E(B-V) = 0.10$). We note that the brightest stars in M48 are saturated in the UVOT data, so we can only give an upper limit. However, the curvature of the upper MS is consistent with an age of ∼300 Myr.

3.4.33. NGC 2567

Positioned slightly above the Galactic midplane, NGC 2567 is a third-quadrant cluster. It has not been the subject of individual study. The K16 study provides basic parameters, identifying the clusters as being of intermediate age (400 Myr) with modest foreground reddening ($E(B-V) = 0.13$), while Conrad et al. (2014) identified it as slightly metal-poor ([Fe/H] = −0.08).

The CG18 selection showed very few member stars. However, our analysis, using the methods of Section 3.4.11, identifies a tight clump of stars in the VPD at the center of the field star distribution. Lowering the probability threshold to 50% selects stars that form a clear MS and MSTO within the CMD (Figure 12, fourth column). We find that the literature parameters exactly reproduce the color–magnitude sequence.

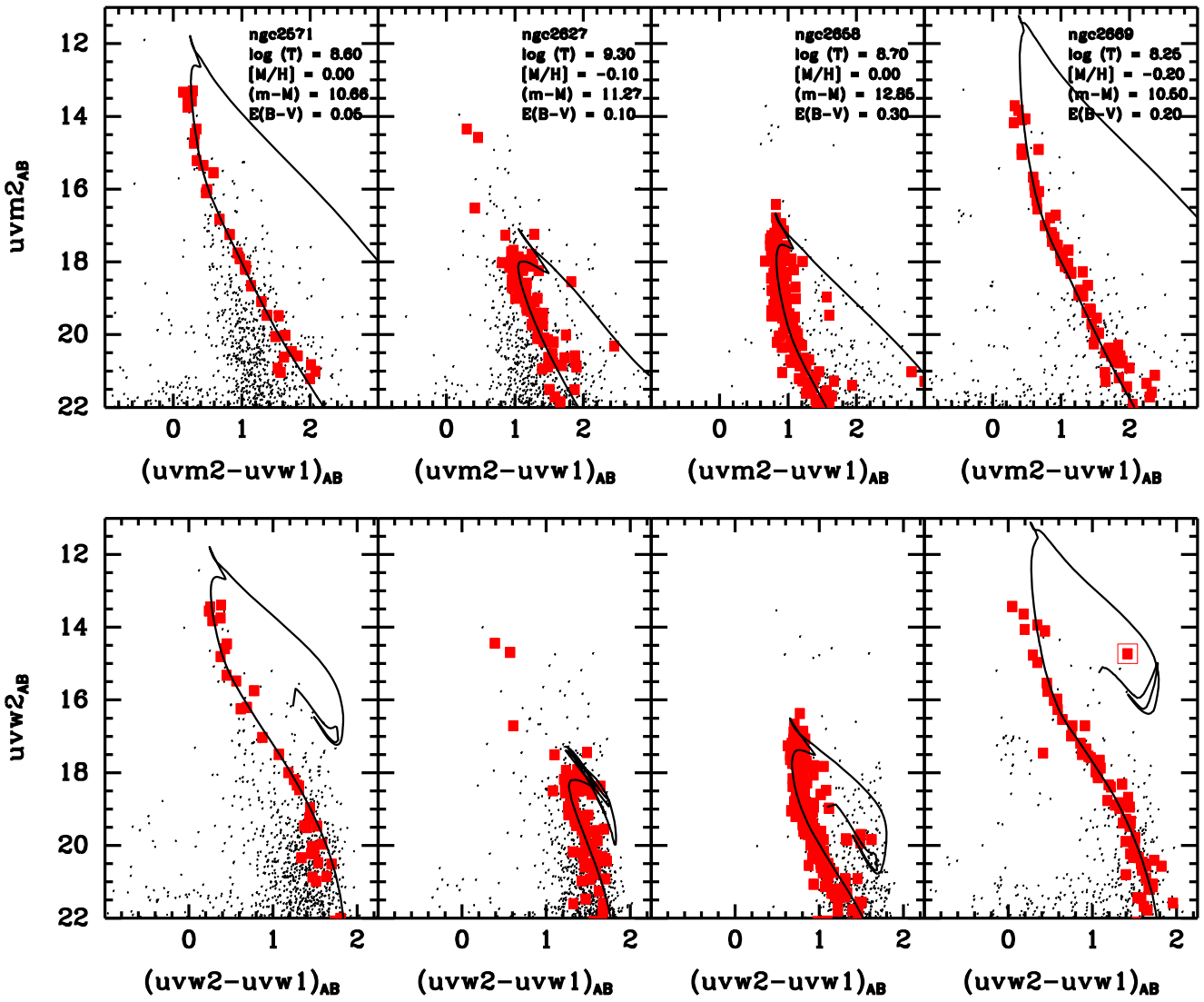

Figure 13. The CMDs of the open clusters NGC 2571, NGC 2627, NGC 2658, and NGC 2669 (left to right). The solid lines are PARSEC-COLIBRI isochrones set to the parameters in the text. Filled red squares show astrometric members selected from *Gaia* DR2 by CG18, while open squares are spectroscopic members from either MMU or sources given in the text.

3.4.34. NGC 2571

Positioned above the midplane, NGC 2571 is a third-quadrant cluster. It has been analyzed by Giorgi et al. (2002) and Özeren et al. (2014). The latter, based on 2MASS photometry, shows moderate reddening ($E(B-V) = 0.36$), while the former shows a small amount of foreground reddening ($E(B-V) = 0.10$). Both agree that the cluster is quite young ($\sim$50 Myr).

The CMD (Figure 13, first column) shows a clean MS that is well separated from the disk. We find, however, that the parameters derived by previous investigators are somewhat inconsistent with the NUV photometry. The high reddening value derived by Özeren et al. (2014) would be inconsistent with the color of the upper MS for any age, predicting a $uvm2 - uvw1$ color several tenths of a magnitude redward of the photometry. The very young ages derived by the previous studies are also inconsistent with the curvature of the upper MS and the brightness and color of the MS. While we have multiple saturated stars in the field, and our age thus represents an upper limit, we note that Kilambi (1978) derived an age of 175 Myr based on photographic photometry, a result that is far more consistent with the NUV photometry we present here. We therefore find it unlikely that this cluster is very young.

3.4.35. NGC 2627

Situated just above the Galactic midplane, NGC 2627 is a third-quadrant cluster. Prior photometric studies have derived an old age of 1.6 Gyr (Piatti et al. 2003; Ahumada 2005). There is no spectroscopic metallicity, but Piatti et al. estimated that is slightly subsolar ([Fe/H] ~ -0.1) based on Washington indices.

Though MMU surveyed the cluster, none of their four RGB stars are detected in the *Swift* data. The astrometric selection, however, produces a clear CMD with a well-defined MS and MSTO (Figure 13, second column). The best-fit isochrone roughly corresponds to the parameters from Ahumada. Note that because of the age, distance, and reddening of this cluster, the RGB/AGB region overlaps the MSTO in the $uvw2 - uvw1$ region. The actual MSTO is the faintest of these loops. Several

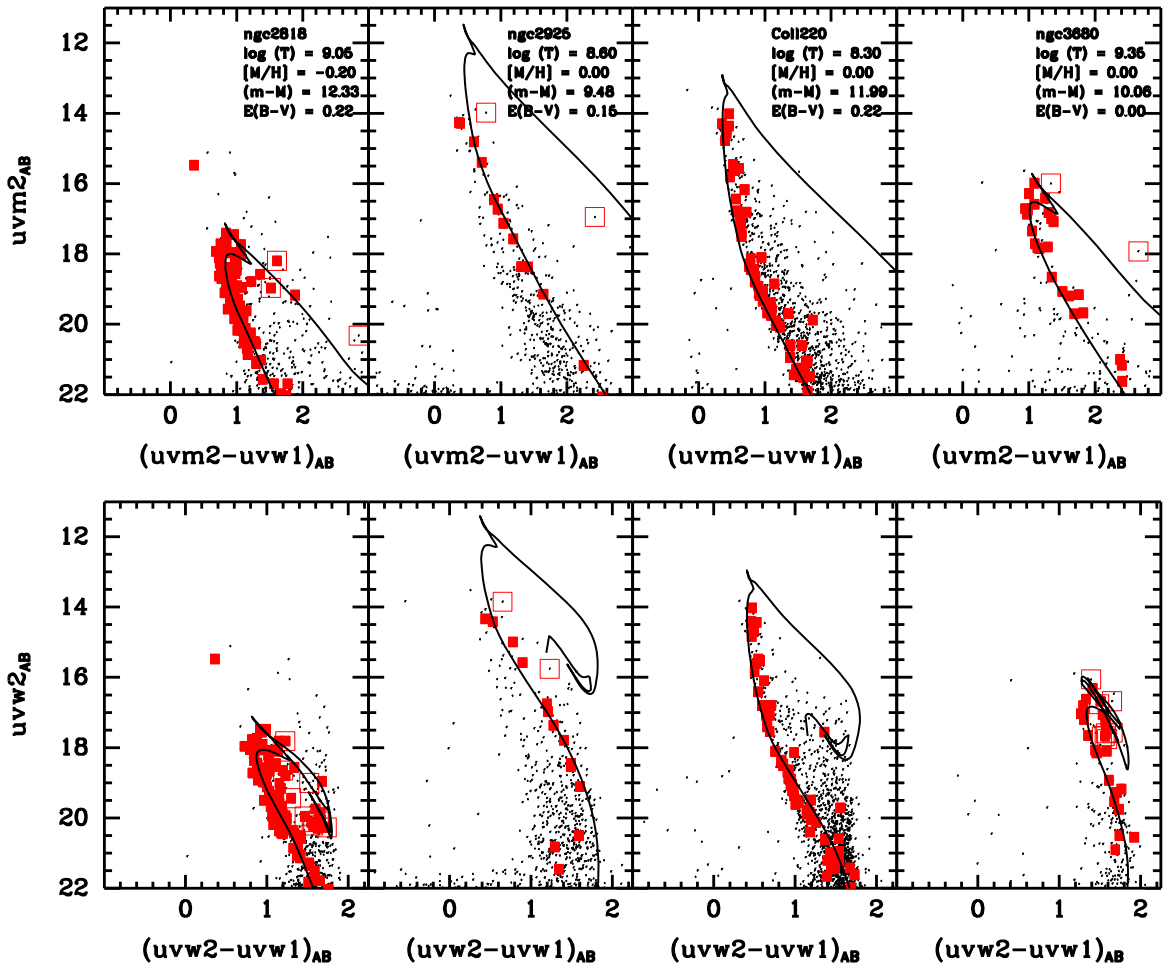

Figure 14. The CMDs of the open clusters NGC 2818, NGC 2825, Collinder 220, and NGC 3680 (left to right). The solid lines are PARSEC-COLIBRI isochrones set to the parameters in the text. Filled red squares show astrometric members selected from *Gaia* DR2 by CG18, while open squares are spectroscopic members from either MMU or sources given in the text.

astrometric members are in the blue straggler region of the CMD, indicating a likely association.

3.4.36. NGC 2658

Located 6° above the Galactic midplane, NGC 2658 is a third-quadrant cluster. The cluster has not been the target of spectroscopic study. Paunzen et al. (2010) indicated that it was metal-poor, but the updated survey of Netopil et al. (2016) indicated solar metallicity. Photometric studies (Ramsay & Pollaco 1992; Ahumada 2003) describe it as of intermediate age (300 Myr) with solar metallicity and moderate reddening ($E(B-V) = 0.40$), making it one of the few significantly reddened clusters in our sample.

The CMDs show a prominent MS and MSTO (Figure 13, third column). Fitting the M17 isochrones to this sequence results in parameters similar to those of the literature, with a slightly lower reddening value of $E(B-V) = 0.30$. The MS does show a significant breadth and some extension beyond the MSTO. This could indicate that it has an eMSTO.

3.4.37. NGC 2669

Located 6° below the Galactic midplane, NGC 2669 is a poorly studied third-quadrant cluster. The last focused study of the cluster was Vogt & Moffat (1973), but it has been included in the global surveys of Paunzen et al. (2010), K13, and K16. These studies hint at a young (100 Myr), slightly metal-poor ($[\mathrm{Fe/H}] \sim -0.20$), moderately reddened ($E(B-V) = 0.18$) cluster.

The astrometric selection includes one MMU radial velocity member and traces the bluer sequence in the CMDs (Figure 13, fourth column). Assuming the Paunzen et al. metallicity, we find parameters similar to those in the literature. We note, however, that the brightest stars are saturated, so the age given is an upper limit.

3.4.38. NGC 2818

Situated above the Galactic midplane, NGC 2818 is a distant third-quadrant cluster. An extensive radial velocity membership is given by MMU. This cluster was recently studied in great detail by Bastian et al. (2018), who found that it has a prominent eMSTO. Their complementary radial velocity study showed that stars on the red side of the eMSTO were fast rotators compared to stars on the blue side, confirming the hypothesis of stellar rotation as the origin of the eMSTO.

The CMDs (Figure 14, first column) show a well-defined MS with a prominent MSTO. We find that the cluster is a bit older than the previous studies, with the MSTO corresponding to an age of approximately 1 Gyr with a slightly lower reddening than Bastiat et al. (2018) of $E(B-V) = 0.15$. One

key difference may be that Bastiat et al. assumed solar metallicity, while we assume a metallicity of [M/H] = −0.2 based on the analysis of Mermilliod et al. (2001). Increasing the [M/H] to solar metallicity would not affect the distance or reddening but would reduce the age of the cluster slightly to 900 Myr. We identify one member star beyond this turnoff that could be either a blue straggler or a disk contaminant.

As noted, Bastian et al. identified an eMSTO in this cluster. As with NGC 2360, the overlap of the convective hook, RGB, and MSTO make analysis tricky. However, the *uvm*2 − *uvw*1 diagram shows that the MSTO is broader and more structured (showing what looks like a bifurcated MSTO) than one would expect from a simple stellar population. Figure 15 shows a close-up of this turnoff region, and it appears to confirm the broadening of the MSTO.

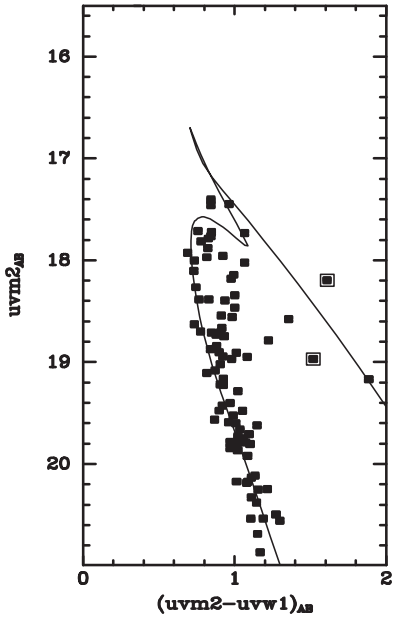

Figure 15. Close-up of the MSTO region of NGC 2818. The panel shows *Gaia*- and spectroscopically selected members. The MSTO region is very broad due to the combination of the eMSTO, convective hook, and beginning of the RGB. The panel shows a broad pattern in the MSTO region, consistent with an eMSTO in NGC 2818 likely resulting from differences in stellar rotation among the MSTO stars.

3.4.39. NGC 2925

Situated just below the Galactic midplane, NGC 2925 is a fourth-quadrant cluster. The only focused study is that of Topaktas (1981), who concluded that the cluster was moderately reddened ($E(B-V) = 0.08$) based on photographic photometry. An intermediate age of 500 Myr was estimated by K16.

While the astrometric selection produces a clean sequence in the CMD (Figure 14, second column), we note that the three RGB stars cross-identified from MMU lie outside of the astrometric selection (two of which are detected by UVOT). In proper-motion space, they span a range of 5 mas yr^{-1}, which is in stark contrast to other clusters, in which spectroscopically confirmed members span at most a few tenths of a mas yr^{-1}. Applying our own analysis to the *Gaia* data results in an almost identical membership selection to CG18 and confirms that the three MMU members are outliers. We therefore find it likely that the MMU stars are not members of NGC 2925 but, given the high proper motions, are halo contaminants. The astrometric members favor the redder sequence in the field. Fitting the M17 isochrones produces a fit very similar to K16 but with an increase in reddening to $E(B-V) = 0.15$.

3.4.40. Collinder 220

Collinder 220 is a fourth-quadrant cluster within the Galactic midplane. It has not been the subject of any published individual study, and our parameters in Table 2 are taken from K16. The UVOT obtained very deep imaging of this cluster due to its proximity to 1E1024.0–5732 (WR21a), a colliding wind binary near the Westerlund 2 cluster that was intensely monitored through periastron.

Analysis of this cluster proved challenging. The VPD shows a clear tight clump of stars within the field star distribution. However, the field is so dense that our double Gaussian modeling failed. Picking out stars in this clump by hand showed (1) a tight sequence of stars in the CMD (Figure 14, third column), (2) a concentration of stars at the nominal position of the cluster, and (3) a mean proper motion roughly consistent with the K13 parameters ($(\mu_\alpha, \mu_{\rm delta}) \sim (-7.3, 2.6)$ compared to (−5.9, 2.5) of K13). The analysis of CG18 identifies most of the same stars as members, albeit with a more conservative selection. We are therefore confident that this is indeed the cluster sequence.

The derived parameters are markedly different from those of K16. We measure a much longer distance ($m-M = 11.99$) and a younger age (200 Myr). What is really interesting about this cluster, however, is that it is the first to require a change in the reddening law in order to properly fit the color–magnitude sequences. Most of our clusters were picked to have low foreground extinction, and even those with more extinction are usually well fit by the standard Milky Way law. However, using the Milky Way law on Collinder 220 produces a discrepancy in the colors of the two MSs that no combination of parameters could fit. Adopting the LMC extinction law, by contrast, results in a consistent fit for both CMDs. Given the disagreement between our measured parameters and those of K16, we put forward this interpretation with caution. However, spectroscopic or multiwavelength study of Collinder 220 would seem warranted to confirm or refute any changes in the UV extinction law toward the cluster.

3.4.41. NGC 3680

Placed slightly above the Galactic midplane, NGC 3680 is a fourth-quadrant cluster. It has been the subject of detailed abundance studies (Santos et al. 2009; Peña Suárez et al. 2018), as well as photometric investigations (Anthony-Twarog & Twarog 2004) that have described it as an old (1.75 Gyr) near-solar metallicity disk cluster.

The astrometric selection produces a clear MS that contains all of the MMU radial velocity members (Figure 14, fourth column). The isochrones, however, favor a solution with minimal or no reddening, which produces a consistent fit with a slightly shorter distance ($m-M = 10.06$) and an older age of 2.2 Gyr.

3.4.42. Lynga 2

Lynga 2 is a small obscured cluster situated toward the Galactic center. The cluster has been poorly studied, likely due

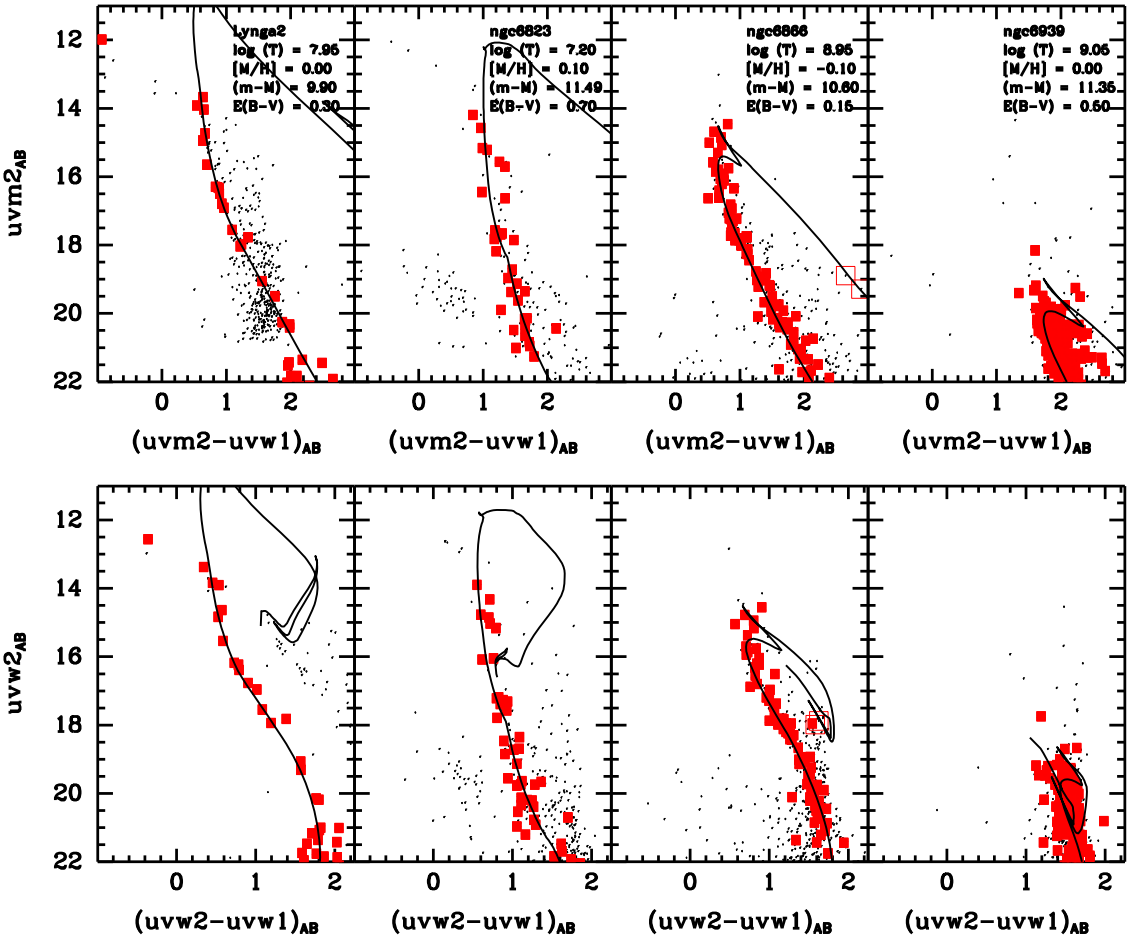

Figure 16. The CMDs of the open clusters Lynga 2, NGC 6823, NGC 6866, and NGC 6939 (left to right). The solid lines are PARSEC-COLIBRI isochrones set to the parameters in the text. Filled red squares show astrometric members selected from *Gaia* DR2 by CG18, while open squares are spectroscopic members from either MMU or sources given in the text.

to the high density of field stars against a relatively spartan cluster. Alter et al. (1970) and Bica et al. (2006) described it as young (90 Myr), with moderate reddening ($E(B-V) = 0.22$).

The astrometric and spectroscopic selection produces a spartan but clear MS in the CMDs (Figure 16, first column). We find that an isochrone using the parameters of Bica et al. follows the color–magnitude sequence quite well (assuming solar metallicity). We note, however, that the brightest member stars are saturated; therefore, we are only able to apply an upper limit to the age of the cluster.

3.4.43. NGC 6823

Situated near the midplane, NGC 6823 is a distant obscured first-quadrant cluster. It is the only very young ($t < 20$ Myr) cluster in our program that is well observed, although it still has a number of saturated stars. It has not been the subject of individual study, so parameters are taken from K16.

The astrometric selection produces a clean, if spartan, MS (Figure 16, second column). Adjusted to lower reddening ($E(B-V) = 0.70$) and longer distance ($m-M = 11.49$) than given in K16, we get excellent agreement between the isochrone and the sequence. The MS is a bit broader than the photometric errors, possibly indicating differential reddening or the influence of stellar rotation. The brightest stars in this cluster are saturated, so only an upper limit on the age can be given. However, this upper limit is close to the K16 age. Given the high-quality data, young age, and foreground extinction, this cluster would be a good candidate for future spectroscopic study.

3.4.44. NGC 6866

Situated within the Galactic midplane, NGC 6866 is a first-quadrant cluster. Previous studies have shown it to be of intermediate age (900 Myr), moderately reddened ($E(B-V) = 0.16$), and slightly metal-poor with $[Fe/H] = -0.10$ (Janes et al. 2014; Bostancı et al. 2015)

The CG18 selection provided to be too conservative—identifying very few cluster members—so we applied our own astrometric selection (Section 3.4.11). The VPD shows a clear clump at the edge of the field star distribution that includes the two MMU radial velocity members and produces a clear MS (Figure 16, third column). Fitting the M17 isochrones to the sequence produces parameters similar to previous investigations.

3.4.45. NGC 6939

Positioned 12° above the Galactic midplane, NGC 6939 is a second-quadrant cluster. Numerous studies have been done of the cluster and have found it to be of solar abundance (Jacobson et al. 2007), heavily reddened ($E(B-V) = 0.33$), and old, with an age of 1.3–1.6 Gyr (Rosvick & Balam 2002;

Andreuzzi et al. 2004). However, there are significant disagreements between the exact parameters derived from the studies, as shown in Table 2.

The astrometric selection identifies a faint MS in the CMDs (Figure 16, fourth column). We find that we can fit this sequence using parameters similar to those of Andreuzzi et al. (2004), but only with some additional reddening ($E(B-V) = 0.50$). This is one of the few clusters in our sample that has substantial reddening, and it is impossible to line up the MS in both color panels without increasing the reddening. At this level of extinction, the $uvw2 - uvw1$ isochrones show portions of the subgiant and giant branch to be bluer than the MSTO because we are only measuring the degree of red leak in these cool and heavily reddened stars. The CMD also shows at least one star that is bluer and brighter than the MSTO. This is a proper-motion member and is located crudely along the MS that a younger stellar population would follow. It is likely that it is a blue straggler.

3.4.46. NGC 6991

The only estimates of the age and distance of NGC 6991, a poorly studied first-quadrant midplane cluster, come from the global survey of K16. Casamiquela et al. (2016) studied the radial velocity but did not measure metallicity. The cluster is quite large (K13 measured a radius of 26.′7); thus, we only image the central regions.

The first column of Figure 17 shows the CMDs of the cluster. The *Gaia* astrometry matches a radial velocity member from Casamiquela et al. (2016). These stars define a narrow CMD sequence. We measure parameters similar to those of K16 but with an older age (1.6 Gyr).

3.4.47. NGC 7058

Located within the Galactic midplane, NGC 7058 is a nearby sparse second-quadrant cluster. It has not been the target of individual study, with the only estimates of its age, distance, and reddening from the global survey of K16.

The CG18 selection found very few member stars, and we therefore applied our method (Section 3.4.11). The VPD shows a clear clump of stars well outside of the field star distribution. This clump corresponds to a sequence in the CMD that reveals NGC 7058 to have—under the assumption of solar metallicity—parameters similar to K16 (Figure 17, second column). We estimate an age of 1.4 Gyr, but this is likely an upper limit. The cluster is sparse, and the images show a small number of bright saturated stars, at least two of which have the same proper motion as the cluster. We note that NGC 7058 is another cluster that shows a deviation from the isochrones for faint stars in the $uvw2 - uvw1$ CMD.

3.4.48. NGC 7063

Situated 9° below the Galactic midplane, NGC 7063 is a first-quadrant cluster. The only comprehensive study to date is that of Peña et al. (2007), who characterized it as young (140 Myr) and with low foreground reddening ($E(B-V) = 0.05$). The MMU survey observed two stars but classified both as nonmembers.

The CG18 selection proved too conservative, and we therefore applied our methods (Section 3.4.11). The VPD shows a clear clump of stars outside of the field star distribution. This clump corresponds to a sequence in the CMD that reveals NGC 7063 to be—under the assumption of solar metallicity—roughly consistent with the parameters of Peña et al. 2007 (Figure 17, third column). We caution that our estimated age is again an upper limit, given the presence of several saturated stars and the curvature of the upper MS. As with other clusters, NGC 7063 shows a deviation from the isochrones for faint stars in the $uvw2 - uvw1$ CMD.

3.4.49. NGC 7209

Positioned 7° below the Galactic midplane, NGC 7209 is a second-quadrant cluster. No spectroscopic metallicity has been published, but photometric studies describe the cluster as being of solar metallicity, intermediate age (500 Myr), and moderately reddened, with $E(B-V) = 0.17$ (Vansevicius et al. 1997; Paunzen et al. 2010; Netopil et al. 2016; K16).

The astrometric and spectroscopic selection finds a clear MS in the CMDs (Figure 17, fourth column). Fitting the M17 isochrones to this sequence yields parameters similar to the literature. However, we note that the CMD shows significant structure that almost resembles a second turnoff. Increasing the age of the cluster to 700 Myr would match this second turnoff, albeit with some slight discrepancy in the curvature of the upper MS. This would relegate the brighter stars to being blue stragglers. If the brighter stars represent the MSTO, then NGC 7209 would have an age of 500 Myr but an eMSTO. Spectroscopic investigation of the rotation rates could determine if this is the case.

4. Discussion

4.1. Isochrones and Cluster Fits

The purpose of this program was to test the utility of standard isochrones in the UV. In that sense, we find that the isochrones perform quite well, successfully reproducing the upper MS for clusters up to several Gyr in age. Most of the CMDs are well described using isochrones set to values at or near those in the literature. For clusters with significant revisions, the source of the discrepancy is either older studies or, in some cases, previous studies mistaking the disk sequence for the cluster sequence.

The consistency between the models and the data shows that even for fairly young stellar populations, the NUV emission is well described by the existing atmospheric models. There is little evidence of stochastic variation and the excess emission produced by chromospheric activity as seen in the FUV (see discussion in Smith 2018). However, it is important to note that our study is focused only on a limited range of parameter space. Almost all of our clusters are older than 100 Myr, and the brightest stars in the youngest are few and saturated. Younger clusters will host much more massive stars, in which factors like binarism, rotation, and magnetic field can play a more important role and our understanding of convention and mixing are poor (see, e.g., Viallet et al. 2013). In addition, our stars are primarily metal-rich (or assumed to be), so we are unable to test how the isochrones perform at lower metallicity levels. Finally, almost all of our clusters are minimally reddened, with only a handful having significant extinction. Unfortunately, these limitations cannot really be exceeded with the Milky Way's contingent of open clusters (at least not using UVOT data). We are currently investigating the UV properties of old metal-poor populations in globular clusters. But exploring very young (<100 Myr) stellar populations or populations with significant

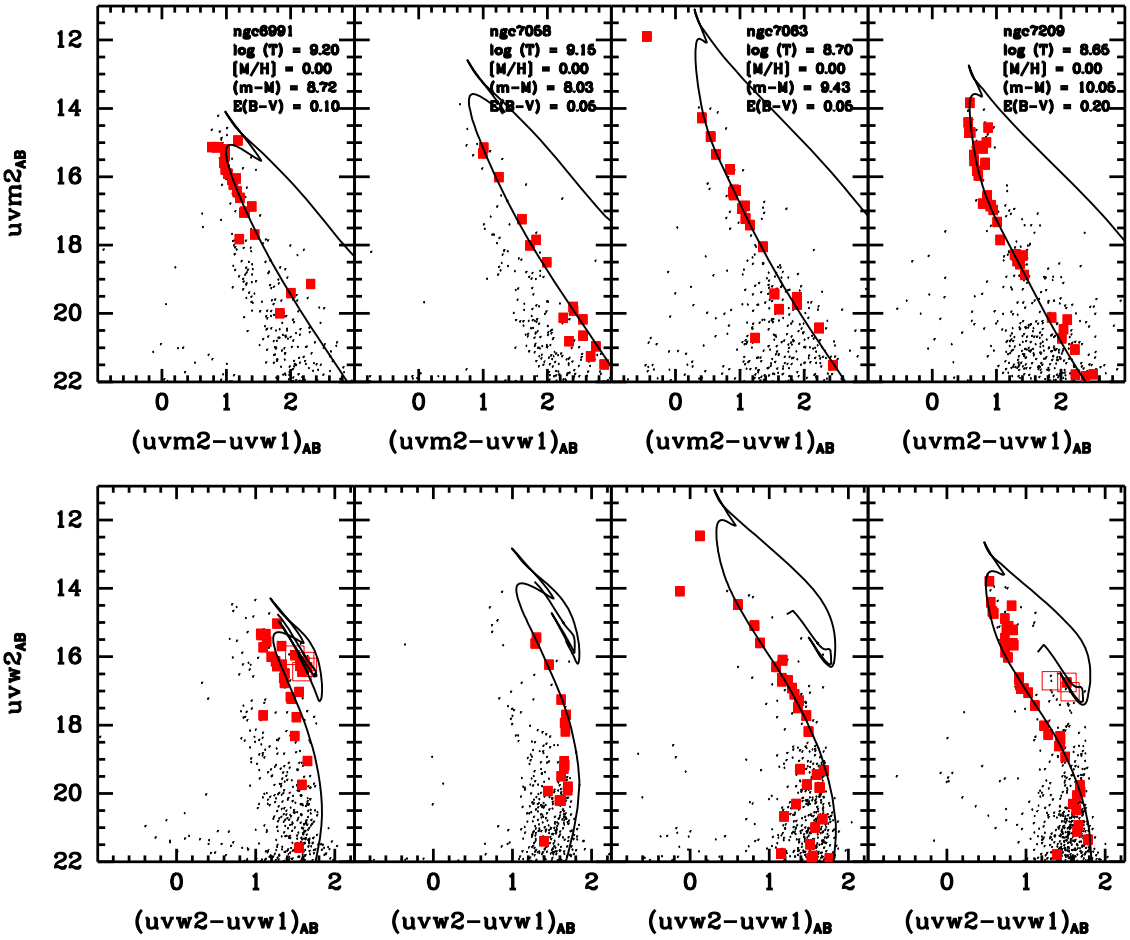

Figure 17. The CMDs of the open clusters NGC 6991, NGC 7058, NGC 7063, and NGC 7209 (left to right). The solid lines are PARSEC-COLIBRI isochrones set to the parameters in the text. Filled red squares show astrometric members selected from *Gaia* DR2 by CG18, while open squares are spectroscopic members from either MMU or sources given in the text.

reddening would require surveys of the nearby stellar populations in the Magellanic Clouds. *Swift*/UVOT has also surveyed these areas (Hagen et al. 2017), but its reach may exceed its grasp in such dense star-forming regions as 30 Doradus, where the younger stars tend to reside. That is more properly the domain of future missions that have the wide-field, high-resolution, multifilter FUV imaging needed to unravel these remaining mysteries.

The main deficiencies in the isochrones are for redder stellar types: the RGB, AGB, and lower-MS stars that are cool and have little emission in the UV. This is hardly a surprise, given that for cool stars (those with $T_{\rm eff} < 7000$ K), the "UV" signal in two of *Swift*'s filters becomes dominated by the red leak. This plays havoc with the effective wavelength (see, e.g., Siegel et al. 2012) and causes the reddening to have a nonlinear effect (Paper I; Brown et al. 2010). For later stellar types that are heavily extinguished, this will cause them to move blueward in $uvw2 - uvw1$ CMDs as the $uvw1$ red leak ramps up faster than the $uvw2$ red leak.

However, it could also be produced by deficiencies in either the isochrones or the underlying atmospheric models. Such discrepancies have been noted before in NUV photometry of cool stars (see, e.g., Barker & Paust 2018) and are likely the result of the underlying atmospheric models having an incomplete treatment of UV absorption lines for very cool atmospheres. This problem has been discussed in detail in the context of the UVBLUE project by Rodríguez-Merino et al. (2005, 2009) and Chavez et al. (2007) and is part of the motivation for the *Hubble Space Telescope*'s upcoming *Hubble* UV Legacy Library of Young Stars as Essential Standards (ULLYSES) program.

To determine the nature of these discrepancies, we examined the deviations of stellar measures from the fit isochrones. This deviation was calculated by measuring, for each star, the minimum quadrature color–magnitude distance from the isochrone. Figure 18 shows the residuals plotted against observational $uvw2 - uvw1$ color and the effective temperature implied by the isochrone. If the problem arises from the red leak, it should occur at a consistent observed color, where the red leak takes over the signal. However, if the problem arises from atmospheric models, it should occur at a consistent effective temperature, where the atmospheric models begin to fail. For clusters that show the deviation at faint magnitudes, the discrepancies do not track the observed stellar color very well. The deviations do, however, track the effective temperature quite well, beginning to deviate toward bluer colors at approximately log $T_{\rm eff} \sim 3.8$, or 6300 K. This hints that the problem lies within the stellar atmospheric models. However, for the bulk of stars that are of interest in the UV, the atmospheric models and isochrones hold up quite well.

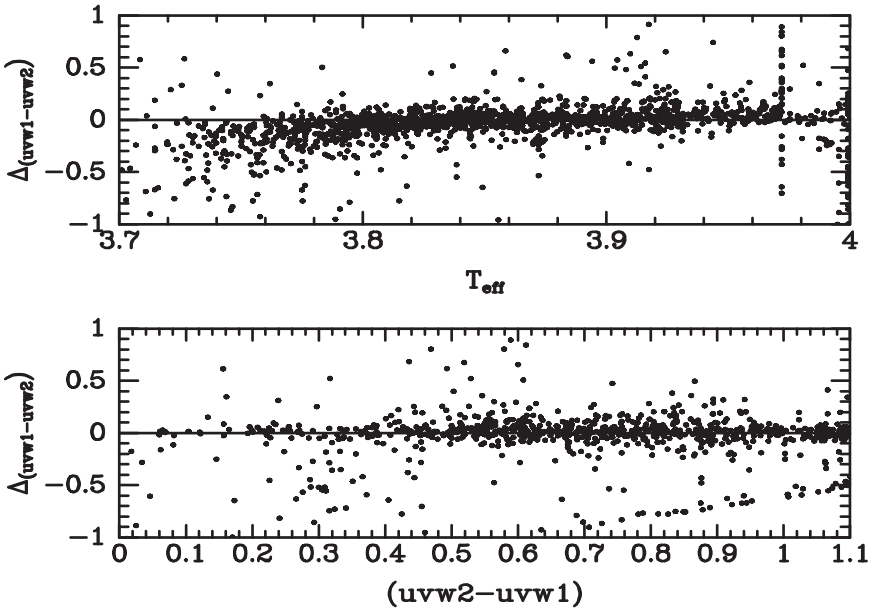

Figure 18. Comparison of photometric distance from the fit isochrones for a sample of the UVOT cluster stars, plotted against absolute $T_{\rm eff}$ (bottom) and observational *uvw*2 − *uvw*1 color (top). The solid line shows agreement. The vertical streak in the top panel is NGC 2658, where the MS is cut off slightly fainter than the blue straggler sequence.

4.2. Reddening Law

As noted above, most of our program clusters have low intrinsic reddening. Those few that have substantial reddening seem to work fine with a "Milky Way"–like extinction law (i.e., one with a shallower slope and a strong 2175 Å bump). Only one cluster—Collinder 220—shows any sign of deviation from the standard reddening law. This is somewhat surprising, as previous investigations have shown some variation in the extinction law at high latitudes within the Galaxy (Peek & Schiminovich 2013) and at low latitudes within the Galaxy (Siegel et al. 2012) and in nearby galaxies (Hagen et al. 2017, 2019). This suggests that future endeavors should look at both the resolved stellar population in nearby galaxies where the reddening law is known to vary and more reddened clusters within our own Galaxy where variations in the law will be amplified and more readily detectable. It might also be of benefit to make these studies multiwavelength, as in Hagen et al. (2017, 2019), where the more well-understood OIR extinction law can be used to "nail down" the line-of-sight extinction, freeing the UV to focus more on variation in the law instead of variation in the total extinction level along the line of sight.

4.3. eMSTOs

Two of our clusters—NGC 2360 and NGC 2818—have previously been identified as having eMSTOs based on photometric and spectroscopic exploration. We confirm the photometric broadening and further note that a number of other clusters (NGC 2355, NGC 2420, NGC 2658, NGC 6823, and NGC 7209) show a similar broadening of the MSTO beyond what is expected from photometric error. This is unlikely to be the effect of differential reddening because most of our clusters were selected to have low reddening, and differential reddening would broaden the entire MS. Spectroscopic investigation of rotation rates would confirm the nature of these eMSTOs, as it has for NGC 2360 and NGC 2818. If confirmed, this would support the contention of Cordoni et al. (2018) that the feature is not unusual among Galactic open clusters and the UV may be more sensitive to the effect than the optical or IR.

Considering that the eMSTO involves the brightest stars in any specific population, this is an effect that may need to be accounted for in spectral synthesis models. While the precise effect of stellar rotation on integrated light is beyond the scope of this paper, the indications that stellar rotation can increase both mass-loss rates and MS lifetime makes their potential ubiquity in young stellar populations critical to both confirm and incorporate into the models.

5. Conclusions

We have measured the photometry of stars in 103 open clusters using the *Swift*/UVOT telescope. We have analyzed 49 of these clusters using *Gaia* DR2 and spectroscopic studies to separate member stars from the field to study precise CMDs and compared the CMDs to theoretical isochrones. Our main results are as follows.

1. The theoretical isochrones reproduce the features of the CMDs very well. The only consistent discrepancy is at faint magnitudes, where cool late-type stars are bluer in *uvw*2 − *uvw*1 space than anticipated. This could be a result of a red leak or inadequacies in the UV opacities in model atmospheres for late-type stars. The discrepancies seem to be more closely related to stellar temperature than observed photometric color, favoring a problem with the model atmospheres.
2. Using these isochrones, we measure age, reddening, and distance for 49 clusters with well-defined color–magnitude sequences. For those that have been studied in detail before, we generally find agreement with literature values. However, there are a number of clusters for which we find significantly different values than the literature, particularly in the third Galactic quadrant, where some previous studies have mistaken the disk sequence for the cluster. We catalog substantially revised parameters for the clusters NGC 2304, NGC 2343, NGC 2360, NGC 2396, NGC 2428,

NGC 2509, NGC 2533, NGC 2571, NGC 2818, Collinder 220, and NGC 6939.
3. We confirm the presence of an eMSTO in two previously studied clusters: NGC 2360 and NGC 2818. We also identify broad MSTO features in at least five other clusters that could warrant further spectroscopic investigation.
4. Most of our clusters have minimal reddening and are thus unsuited to probe the UV properties of the foreground dust. However, one cluster, Collinder 220, shows significant improvement in the isochrone fits if an "LMC-like" reddening law—one with a smaller red bump at 2175 Å and a steeper extinction curve—is used.

Our investigation has only scratched the surface of what this remarkable data set can yield. Measuring the integrated light would allow direct comparison between isochrones and synthetic spectral models to test the validity of the latter for unresolved stellar populations. Combining this database with extra ground-based optical photometry or the broadband photometry of *Gaia* DR2 would allow the detection of unresolved white dwarf–MS binaries, providing additional insight into the role of binarism in spectral synthesis models and the integrated luminosity of the stellar population (see, e.g., Buzzoni et al. 2012; Hernández-Pérez & Bruzual 2013). A more thorough examination of the MSTOs—especially in combination with spectroscopic study—would allow a much more detailed exploration of eMSTOs and their connection to cluster age.

The authors acknowledge sponsorship at PSU by NASA contract NAS5-00136. This research was also supported by the NASA ADAP through grants NNX13AI39G and NNX12AE28G. The authors thank L. Girardi for useful discussions about the NUV isochrones. The Institute for Gravitation and the Cosmos is supported by the Eberly College of Science and the Office of the Senior Vice President for Research at the Pennsylvania State University.

ORCID iDs

Lea M. Z. Hagen https://orcid.org/0000-0001-8918-1597

References

Ahumada, J. A. 2003, RMdAA, 39, 41
Ahumada, J. A. 2005, AN, 326, 3
Ahumada, J. A., & Lapasset, E. 2007, A&A, 463, 789
Alter, G., Balazs, B., Ruprecht, J., & Vanysek, J. 1970, Catalogue of Star Clusters and Associations (2nd ed.; Budapest: Akademiai)
Andreuzzi, G., Bragaglia, A., Tosi, M., & Marconi, G. 2004, MNRAS, 348, 297
Ann, H. B., Lee, S. H., Sung, H., et al. 2002, AJ, 123, 905
Anthony-Twarog, B. J., Deliyannis, C. P., & Twarog, B. A. 2016, AJ, 152, 192
Anthony-Twarog, B. J., Lee-Brown, D. B., Deliyannis, C. P., & Twarog, B. A. 2018, AJ, 155, 138
Anthony-Twarog, B. J., Tanner, D., Cracraft, M., & Twarog, B. A. 2006, AJ, 131, 461
Anthony-Twarog, B. J., & Twarog, B. A. 2004, AJ, 127, 1000
Balaguer-Núñez, L., Jordi, C., & Galadí-Enríquez, D. 2005, A&A, 437, 457
Barker, H., & Paust, N. E. Q. 2018, PASP, 130, 034204
Bastian, N., Kamann, S., Cabrera-Ziri, I., et al. 2018, MNRAS, 480, 3739
Bica, E., Bonatto, C., & Blumberg, R. 2006, A&A, 460, 83
Böcek Topcu, G., Afşar, M., Schaeuble, M., & Sneden, C. 2015, MNRAS, 446, 3562
Bostancı, Z. F., Ak, T., Yontan, T., et al. 2015, MNRAS, 453, 1095
Bragaglia, A., Gratton, R. G., Carretta, E., et al. 2012, A&A, 548, A122
Bragaglia, A., Sestito, P., Villanova, S., et al. 2008, A&A, 480, 79
Breeveld, A. A., Landsman, W., Holland, S. T., et al. 2011, in AIP Conf. Proc. 1358, Gamma Ray Bursts, ed. J. E. McEnery, J. L. Racusin, & N. Gehrels (Melville, NY: AIP), 373
Brown, T. M., Sweigart, A. V., Lanz, T., et al. 2010, ApJ, 718, 1332
Bruzual, A. G. 2009, A&A, 500, 521
Burrows, D. N., Hill, J. E., Nousek, J. A., et al. 2005, SSRv, 120, 165
Buzzoni, A., Bertone, E., Carraro, G., & Buson, L. 2012, ApJ, 749, 35
Calzetti, D., Lee, J. C., Sabbi, E., et al. 2015, AJ, 149, 51
Cantat-Gaudin, T., Jordi, C., Vallenari, A., et al. 2018, A&A, 618, A93, [CG18]
Carraro, G., & Chiosi, C. 1994, A&A, 288, 751
Carraro, G., Chiosi, C., Bressan, A., & Bertelli, G. 1994, A&AS, 103, 375
Carraro, G., & Costa, E. 2007, A&A, 464, 573
Carraro, G., Girardi, L., & Chiosi, C. 1999, MNRAS, 309, 430
Carraro, G., Vázquez, R. A., Costa, E., Ahumada, J. A., & Giorgi, E. E. 2015, AJ, 149, 12
Casamiquela, L., Carrera, R., Jordi, C., et al. 2016, MNRAS, 458, 3150
Chavez, M., Bertone, E., Buzzoni, A., et al. 2007, ApJ, 657, 1046
Claria, J. J. 1985, A&AS, 59, 195
Clariá, J. J., Piatti, A. E., Lapasset, E., & Parisi, M. C. 2005, BaltA, 14, 301
Clariá, J. J., Piatti, A. E., Mermilliod, J.-C., & Palma, T. 2008, AN, 329, 609
Conrad, C., Scholz, R.-D., Kharchenko, N. V., et al. 2014, A&A, 562, A54
Cordoni, G., Milone, A. P., Marino, A. F., et al. 2018, ApJ, 869, 139
Daniel, S. A., Latham, D. W., Mathieu, R. D., & Twarog, B. A. 1994, PASP, 106, 281
Davidge, T. J. 2013, PASP, 125, 115
De Martino, C., Bianchi, L., Pagano, I., Herald, J., & Thilker, D. 2008, MmSAI, 79, 704
Dias, W. S., Alessi, B. S., Moitinho, A., & Lépine, J. R. D. 2002, A&A, 389, 871
Dobbie, P. D., Day-Jones, A., Williams, K. A., et al. 2012, MNRAS, 423, 2815
Donati, P., Bragaglia, A., Carretta, E., et al. 2015, MNRAS, 453, 4185
Friel, E. D. 1995, ARA&A, 33, 381
Frinchaboy, P. M., & Majewski, S. R. 2008, AJ, 136, 118
Frinchaboy, P. M., Muñoz, R. R., Phelps, R. L., Majewski, S. R., & Kunkel, W. E. 2006, AJ, 131, 922
Frogel, J. A., & Twarog, B. A. 1983, ApJ, 274, 270
Gaia Collaboration, Brown, A. G. A., Vallenari, A., et al. 2018, A&A, 616, A1
Gaia Collaboration, Prusti, T., de Bruijne, J. H. J., et al. 2016, A&A, 595, A1
Gehrels, N., Chincarini, G., Giommi, P., et al. 2004, ApJ, 611, 1005
Geller, A. M., Latham, D. W., & Mathieu, R. D. 2015, AJ, 150, 97
Georgy, C., Charbonnel, C., Amard, L., et al. 2019, A&A, 622, A66
Giorgi, E. E., Vàzquez, R. A., Baume, G., Seggewiss, W., & Will, J.-M. 2002, A&A, 381, 884
Glaspey, J. W. 1987, PASP, 99, 1089
Gordon, K. D., Clayton, G. C., Misselt, K. A., Landolt, A. U., & Wolff, M. J. 2003, ApJ, 594, 279
Goudfrooij, P., Puzia, T. H., Kozhurina-Platais, V., & Chandar, R. 2011, ApJ, 737, 3
Hagen, L. M. Z., Siegel, M. H., & Gronwall, C. A. 2019, MNRAS, submitted
Hagen, L. M. Z., Siegel, M. H., Hoversten, E. A., et al. 2017, MNRAS, 466, 4540
Harris, G. L. H., Fitzgerald, M. P. V., Mehta, S., & Reed, B. C. 1993, AJ, 106, 1533
Hasegawa, T., Sakamoto, T., & Malasan, H. L. 2008, PASJ, 60, 1267
Hernández-Pérez, F., & Bruzual, G. 2013, MNRAS, 431, 2612
Hoversten, E. A., Gronwall, C., Vanden Berk, D. E., et al. 2011, AJ, 141, 205
Jacobson, H. R., Friel, E. D., & Pilachowski, C. A. 2007, AJ, 134, 1216
Jacobson, H. R., Pilachowski, C. A., & Friel, E. D. 2011, AJ, 142, 59
Janes, K., Barnes, S. A., Meibom, S., & Hoq, S. 2014, AJ, 147, 139
Jeffery, E. J., von Hippel, T., van Dyk, D. A., et al. 2016, ApJ, 828, 79
Jones, B. F., & Prosser, C. F. 1996, AJ, 111, 1193
Kassis, M., Janes, K. A., Friel, E. D., & Phelps, R. L. 1997, AJ, 113, 1723
Kharchenko, N. V., Piskunov, A. E., Schilbach, E., Röser, S., & Scholz, R.-D. 2013, A&A, 558, A53, [K13]
Kharchenko, N. V., Piskunov, A. E., Schilbach, E., Röser, S., & Scholz, R.-D. 2016, A&A, 585, A101, [K16]
Kilambi, G. C. 1978, PASP, 90, 721
Krisciunas, K., Monteiro, H., & Dias, W. 2015, PASP, 127, 31
Lata, S., Pandey, A. K., Kumar, B., et al. 2010, AJ, 139, 378
Lee, S. H., Kang, Y.-W., & Ann, H. B. 2012, MNRAS, 425, 1567
Mackey, A. D., & Broby Nielsen, P. 2007, MNRAS, 379, 151
Maderak, R. M., Deliyannis, C. P., King, J. R., & Cummings, J. D. 2013, AJ, 146, 143
Marigo, P., Girardi, L., Bressan, A., et al. 2017, ApJ, 835, 77

Marino, A. F., Milone, A. P., Casagrande, L., et al. 2018, ApJL, 863, L33
Meibom, S., Mathieu, R. D., Stassun, K. G., Liebesny, P., & Saar, S. H. 2011, ApJ, 733, 115
Mermilliod, J.-C., Clariá, J. J., Andersen, J., Piatti, A. E., & Mayor, M. 2001, A&A, 375, 30
Mermilliod, J. C., Mayor, M., & Udry, S. 2008, A&A, 485, 303, [MMU]
Milone, A. P., Bedin, L. R., Piotto, G., & Anderson, J. 2009, A&A, 497, 755
Netopil, M. 2017, MNRAS, 469, 3042
Netopil, M., Paunzen, E., Heiter, U., & Soubiran, C. 2016, A&A, 585, A150
Oralhan, İ. A., Karataş, Y., Schuster, W. J., Michel, R., & Chavarría, C. 2015, NA, 34, 195
Özeren, F. F., Arslan, Ö, Küçük, İ., & Oralhan, İ. A. 2014, NewA, 32, 36
Page, M. J., Chan, N., Breeveld, A. A., et al. 2017, MNRAS, 466, 1061
Parisi, M. C., Clariá, J. J., Piatti, A. E., & Geisler, D. 2005, MNRAS, 363, 1247
Park, H. S., & Lee, M. G. 1999, MNRAS, 304, 883
Paunzen, E., Heiter, U., Netopil, M., & Soubiran, C. 2010, A&A, 517, A32
Peek, J. E. G., & Schiminovich, D. 2013, ApJ, 771, 68
Pei, Y. C. 1992, ApJ, 395, 130
Peña, J. H., Fox Machado, L., & Garrido, R. 2007, RMxAA, 43, 329
Peña, J. H., & Martínez, A. 2014, RMxAA, 50, 119
Peña Suárez, V. J., Sales Silva, J. V., Katime Santrich, O. J., Drake, N. A., & Pereira, C. B. 2018, ApJ, 854, 18
Piatti, A. E., Clariá, J. J., & Ahumada, A. V. 2003, MNRAS, 346, 390
Piatti, A. E., Clariá, J. J., & Ahumada, A. V. 2010, MNRAS, 402, 2720
Poole, T. S., Breeveld, A. A., Page, M. J., et al. 2008, MNRAS, 383, 627
Prisinzano, L., Micela, G., Sciortino, S., & Favata, F. 2003, A&A, 404, 927
Ramsay, G., & Pollaco, D. L. 1992, A&AS, 94, 73
Reddy, A. B. S., Giridhar, S., & Lambert, D. L. 2012a, in Astronomical Society of India Conf. Ser. 4, ed. A. Subramanian & S. Anathpindika (Pune: ASICS), 197
Reddy, A. B. S., Giridhar, S., & Lambert, D. L. 2012b, MNRAS, 419, 1350
Reddy, A. B. S., Giridhar, S., & Lambert, D. L. 2013, MNRAS, 431, 3338
Reddy, A. B. S., Giridhar, S., & Lambert, D. L. 2015, MNRAS, 450, 4301
Rider, C. J., Tucker, D. L., Smith, J. A., et al. 2004, AJ, 127, 2210
Rodríguez-Merino, L. H., Cardona, O., Bertone, E., Chávez, M., & Buzzoni, A. 2009, ASSP, 7, 239
Rodríguez-Merino, L. H., Chavez, M., Bertone, E., & Buzzoni, A. 2005, ApJ, 626, 411
Rojo Arellano, E., Pena, J. H., & Gonzalez, D. 1997, A&AS, 123, 25
Roming, P. W., Townsley, L. K., Nousek, J. A., et al. 2000, Proc. SPIE, 4140, 76
Roming, P. W. A., Hunsberger, S. D., Mason, K. O., et al. 2004, Proc. SPIE, 5165, 262
Roming, P. W. A., Kennedy, T. E., Mason, K. O., et al. 2005, SSRv, 120, 95
Rosvick, J. M., & Balam, D. 2002, AJ, 124, 2093
Sales Silva, J. V., Peña Suárez, V. J., Katime Santrich, O. J., et al. 2014, AJ, 148, 83
Santos, N. C., Lovis, C., Melendez, J., et al. 2012, A&A, 538, A151
Santos, N. C., Lovis, C., Pace, G., Melendez, J., & Naef, D. 2009, A&A, 493, 309
Schuler, S. C., King, J. R., Fischer, D. A., Soderblom, D. R., & Jones, B. F. 2003, AJ, 125, 2085
Searle, L., Wilkinson, A., & Bagnuolo, W. G. 1980, ApJ, 239, 803
Seaton, M. J. 1979, MNRAS, 187, 73P
Sharma, S., Pandey, A. K., Ogura, K., et al. 2006, AJ, 132, 1669
Siegel, M. H., Hoversten, E., Bond, H. E., Stark, M., & Breeveld, A. A. 2012, AJ, 144, 65
Siegel, M. H., Porterfield, B. L., Linevsky, J. S., et al. 2014, AJ, 148, 131, [Paper I]
Sindhu, N., Subramaniam, A., & Radha, C. A. 2018, MNRAS, 481, 226
Smith, G. H. 2018, PASP, 130, 084206
Souto, D., Cunha, K., Smith, V., et al. 2016, ApJ, 830, 35
Stecher, T. P. 1965, ApJ, 142, 1683
Stetson, P. B. 1987, PASP, 99, 191
Stetson, P. B. 1994, PASP, 106, 250
Sujatha, S., & Babu, G. S. D. 2003, BASI, 31, 9
Tadross, A. L. 2005, JKAS, 38, 357
Tapia, M. T., Schuster, W. J., Michel, R., et al. 2010, MNRAS, 401, 621
Topaktas, L. 1981, A&AS, 45, 111
Twarog, B. A., Anthony-Twarog, B. J., Deliyannis, C. P., & Thomas, D. T. 2015, AJ, 150, 134
Twarog, B. A., Ashman, K. M., & Anthony-Twarog, B. J. 1997, AJ, 114, 2556
Vansevicius, V., Platais, I., Paupers, O., & Abolins, E. 1997, MNRAS, 285, 871
Viallet, M., Meakin, C., Arnett, D., & Mocák, M. 2013, ApJ, 769, 1
Vogt, N., & Moffat, A. F. J. 1973, A&AS, 9, 97
von Hippel, T., & Gilmore, G. 2000, AJ, 120, 1384
Wang, K., Deng, L., Zhang, X., et al. 2015, AJ, 150, 161
Wu, Z.-Y., Zhou, X., Ma, J., Jiang, Z.-J., & Chen, J.-S. 2005, PASP, 117, 32
Yong, D., Carney, B. W., & Friel, E. D. 2012, AJ, 144, 95
Yong, D., Carney, B. W., & Teixera de Almeida, M. L. 2005, AJ, 130, 597